Dynamic structural insights to decipher the critical determinant of RORγt binding with Agonist and Antagonist

Shantanu Kumar
Enrolment No: CUSB2203312032

In Partial Fulfilment of
the Requirements for the Degree of

Master of Science in Bioinformatics

Under the Supervision of

Dr. Shailendra Asthana

PRINCIPAL SCIENTIST-II

Computational and Mathematical Biology Center (CMBC)

Translational Health Science and Technology Institute

Submitted to

Department of Bioinformatics

School of Earth, Biological and Environmental Sciences

Central University of South Bihar, Gaya, India

July 2024

Declaration

The work embodied in the thesis entitled '**Dynamic structural insights to decipher the critical determinant of RORγt binding with Agonist and Antagonist**' was carried out by me under the supervision of **Dr. Shailendra Asthana**, PRINCIPAL SCIENTIST-II, in Computational and Mathematical Biology Center (CMBC), Translational Health Science and Technology Institute (THSTI)in partial fulfilment of the requirements for the award of M.Sc. Degree in Bioinformatics. The work has not been submitted in part or full, to this or any other University or Institution, for any Degree or Diploma.

Date: 09/07/2024   **Shantanu Kumar**

Place: Faridabad

Certificate

This is to certify that the thesis entitled **'Dynamic structural insights to decipher the critical determinant of RORγt binding with Agonist and Antagonist'** submitted by **Shantanu Kumar, Enrolment No. CUB2203312032**, in partial fulfilment of the requirements for the award of **M.Sc. Degree in Bioinformatics** of **Central University of South Bihar** has not been previously submitted for the award of any Degree or Diploma of this or any other University or Institution and it is his/her original work.

Date:

Dr. Asheesh Shanker
Professor & Head
Department of Bioinformatics
Central University of South Bihar

Acknowledgment

Among the people whom I am blessed with, I am wishing my first gratitude to my guide **Dr. Shailendra Asthana**, Principal Scientist- II, Computational and Mathematical Biology Center, THSTI for their encouragement, inspiration and guidance throughout the tenure of my dissertation work. It was indeed a matter of privilege for me to have him as my guide. They always provided incessant inspiration, priceless and prudent guidance, much needed constructive criticism, persistent help, support, and above all, the upbeat approach towards my abilities made the achievement of this goal, a learning, rewarding and enlightening experience.

I would like to extend my heartfelt gratitude to **Dr. Mitul Srivastava, Dr. Shilpa Sharma, Dr. Kiran Lokhande, Mr. Debopriyo Shrmadhikari, Mr. Gagandeep Singh, Mr. Abhishek Choudhary, Miss Ridhima, and Mr. Mohit Pareek** for their continuous support and help during my whole dissertation period.

I would like to express my heartfelt gratitude and sincere acknowledgement to the esteemed faculties of the Department of Bioinformatics at the Central University of South Bihar. Their unwavering dedication, valuable teachings, constant guidance, and endless inspiration have played a pivotal role in shaping my academic journey over the past year. I am truly indebted to them for their immense support.

I would also like to extend my deepest appreciation to my family. Words cannot adequately convey the extent of my gratitude for their unrelenting love, encouragement, and unwavering belief in my abilities. Their support has been invaluable, and I am forever grateful for everything they have done for me.

Shantanu Kumar

LIST OF CONTENTS

Abbreviations

ROR	Related Orphan Receptor
RORγt	Retinoic Acid Receptor-Related Orphan Nuclear Receptor Gamma t
NR	Nuclear Receptor
LBD	Ligand Binding Domain
TNF	Tumour Necrosis Factor
DBD	DNA-binding domain
RAR	Retinoic Acid Receptor
RXR	Retinoic X Receptor
SRC2	Steroid Receptor Activator 2
MD	Molecular Dynamics
MMPBSA	Molecular Mechanics-Poisson Boltzmann Surface Area
PDB	Protein Data Bank
AMBER	Assisted Model Building with Energy Refinement
LGA	Lamarckian Genetic Algorithm
MM-GBSA	Molecular Mechanics-Generalized Boltzmann Surface Area
ΔG Bind	Binding Free Energy

List of Tables

List of Fig

Abstract

For structure-based drug discovery, elucidating structural determinants is essential. Th17 cells provide immune-dependent defence against infections and cancer. Th-17 cells' master regulator (Ivanov et al., 2006), RORγt, is activated by small molecule binding at its orthosteric site, which is followed by the recruitment of co-repressors and co-activators in its ligand binding domain (AF-2) (Kanai et al., 2012). The RORγt (Retinoic acid receptor-related orphan nuclear receptor gamma) is a proven target for autoimmune disease, cancer and pathogens.

The selective designing of agonist and antagonist is difficult because they both bind in the same binding site, i.e. the orthosteric site, which is highly dynamic and has interaction with the LBD site. In this study, we examine three different systems, i.e. the apo protein, the protein bounded state with agonist, and the protein bounded state with an antagonist in the orthosteric-binding pocket using molecular docking and molecular dynamic simulations. We found that the orthosteric binding pocket in apo protein of RORγt was mostly open, confirming that apo protein was constitutively active and could be activated by an agonist binding it. As the binding of an agonist helped to stabilize the H12 helix structure of RORγt (Y. Wang et al., 2018). Additionally, we have tried to demonstrate that antagonist binding at the orthosteric binding pocket can disrupt the transcription function of RORγt. After binding of the antagonist, H12 is destabilized by the movement of residue W317 which interrupts the intramolecular interaction between residues of the protein helix. Due to this, H12 becomes flexible or reorients its position.This work provides a new novel structural and mechanistic understanding that is essential for RORγt target drug discovery in designing agonists and antagonists.

Keywords: RORγt, Agonist, Antagonist, Molecular Dynamics Simulation, LBD

1. Introduction

1.1 ROR nuclear receptors

The nuclear receptor (NR) superfamily is composed of a family of transcription factors (TFs) that play an important role in a number of biological processes including metabolism, reproduction, and inflammation (McEwan, 2009). Diseases caused by dysregulation of nuclear receptor (NR) signaling include cancer, diabetes, obesity, and autoimmune disorders. In humans, members of 48 transcription factors are composed of the NR superfamily (Weikum et al., 2018). These members share highly conserved and identical domains. NR proteins consist of six domain functional structures (A-F), comprising the N-terminal Activation Function-1 domain (A/B), followed by a(Kanai et al., 2012) DNA-Binding domain (C), the flexible hinge region (D) and the C-terminal ligand binding domain (LBD) (E/F) (Suri et al., 2022) (Fig. 1).

Its A/B region denotes the amino terminus's ligand-independent activation function 1 (AF-1) domain. Its DNA-binding domain (DBD) is conserved in the C region of the protein with two zinc motifs for binding distinct DNA response elements(Zhang et al., 2015) . The relatively short and flexible D (hinge) region connects the C region to the E region. The E/F region is the carboxy-terminal ligand binding domain (LBD), housing the ligand-dependent activation domain 2 (AF-2). The DBD and LBD regions exhibit the greatest sequence and length similarity within the superfamily, whereas AF-1 and the hinge regions exhibit the greatest differences (Horwitz et al., 1996). The conformation of the LBD is altered upon ligand binding. It alters the surface to help attract cofactor proteins, which control target gene induction or repression transcriptionally (Horwitz et al., 1996) . RORs are involved in various physiological and pathological functions. Due to this, they can be used in the development of clinical treatments for various diseases.

The identification of the ROR family has been revealed in many mammalian species. They express specific tissues depending on different tissue types. The human ROR genes can produce several isoforms of receptors with variations at the C-terminal because of alternative promoter usage and splicing. The first member of this group was identified and named RORα, also known as retinoic acid

receptor-related orphan receptor alpha (RORA) in 1990 (Zhang et al., 2015). This naming was based on its homology to retinoic acid receptor (RAR) and retinoic X receptor (RXR) (Parrado et al., 2001). Subsequently, others identified were RORβ and RORγ. The expression pattern in tissues differs between RORα, β and γ.

1.2 Retinoic-acid-receptor-related orphan nuclear receptor gamma (RORγt)

RORγt that stands for retinoic acid receptor-related orphan nuclear receptor gamma is one of the master regulators in the development of T helper 17 cells (Th17 cells), which are essential for the initiation of many autoimmune diseases such as multiple sclerosis, rheumatoid arthritis, inflammatory bowel disease and psoriasis (Suri et al., 2022). On the other hand, IL-17 released by Th-17 cells protect against certain cancers like melanomas of skin, prostate and breast tumors among others and some disorders associated with inflammation. CD8+ T-cells are stimulated by Th-17 cells. Again these cells produce IL-21 and IL-22 cytokines responsible for initiating protection against infection. RORγt or RORγ is a nuclear receptor found in TH17 cells that is also expressed in thymocytes only (Conti et al., 2009). Only the N-terminal sequences differentiate two isoforms whereas their ligand binding domains (LBD) are identical.

RORγt is involved in the presence of TGFb/IL-1b and IL-6. To upregulate Th17 cell differentiation, tumour necrosis factor (TNF) together with IL-1b collaborates to increase IL-6 production(Zou & Restifo, 2010) . Also, the activated RORγt causes the release of cytokines such as IL-17 and IL-23 while the latter's binding on its receptor, IL-23R further aids in the up-regulation of RORγt by signaling through STAT3 (Khan & Ansar Ahmed, 2015). However, when severely used alone, this particular cytokine does not give rise to differentiated Th17 cells but instead promotes a feedback loop that leads to over-expression of RORγt, TNF, IL-1β and other related genes (Zhu et al., 2010).

1.3 RORγt as a therapeutic target

Th17 cells are involved in the pathogenesis of various inflammatory and autoimmune diseases like Multiple sclerosis, Rheumatoid Arthritis, Psoriasis and many inflammatory conditions. RORγt is a transcription factor that plays a critical role in regulating gene expression necessary for the differentiation and functionality of Th17 cells, a subset of T helper cells (Park et al., 2014) . This key transcription factor is responsible for promoting the differentiation of naïve CD4+ T cells into Th17 cells. RORγt binds to the specific DNA sequence that promotes interleukin-17 (IL-17) (Khan & Ansar Ahmed, 2015)transcription and other pro-inflammatory cytokines. Recent studies suggest that modulating the activity of RORγt and Th17 cells potentially affects cancer immunotherapy(Zou & Restifo, 2010). Secukinumab and Ixekizumab are antibodies that target IL-17, inhibiting its signaling pathway, which is associated with conditions such as psoriasis, rheumatoid arthritis (RA), and uveitis (Blauvelt & Chiricozzi, 2018). Hereby, RORγt can be considered as a therapeutic target for the cure of associated autoimmune diseases due to its eminent role in production of IL-17A and controlling the differentiation of Th17 cells.

1.4 Structure detail of RORγt

In terms of structure, RORγt is closely related to various families of NRs and includes a DNA binding domain (DBD), a N-terminus, a hinge region, and a ligand-binding domain (LBD) at the end (Zhang et al., 2015). The DBD connects to selective DNA binding while LBD acts as an on-off switch for gene transcription. Six domains (A-F) are annotated for this 518 amino acid protein with each individually characterized by sequence similarity to diverse nuclear receptors (Suri et al., 2022). Varied regions are mostly found in the A/B domain and constitutive activation function is found in AF-1. Within the LBD, there are 12 helices; two or three β-sheets is center to ligand binding and houses the AF-2 helix (H12). H12 recruits LXXLL-motif-containing co-activator or corepressor peptide (Kallen et al., 2017).
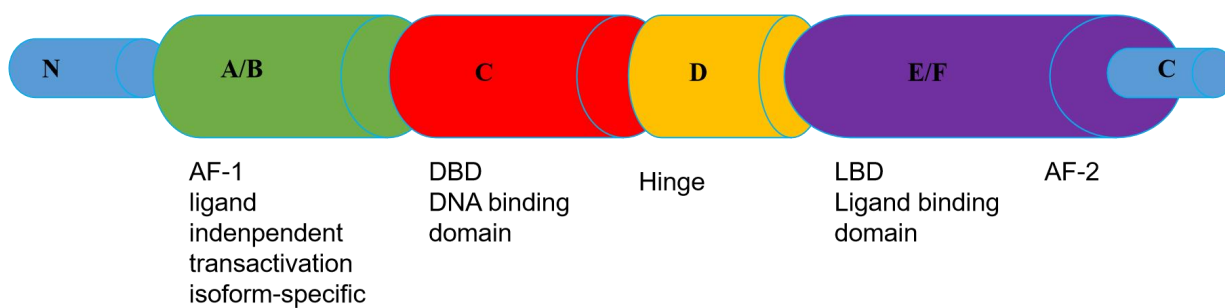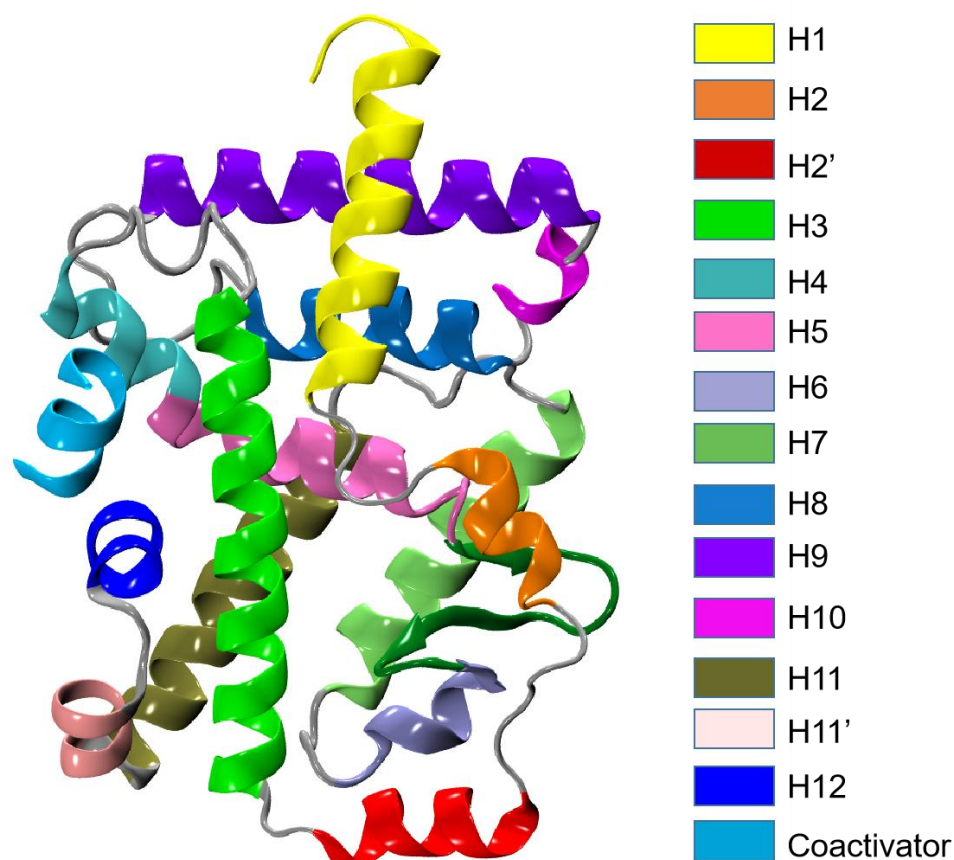
Fig 1. RORγt structure annotation. (A) schematic diagram RORγtdomain, which consists of six domain (A-F), comprising the N-terminal Activation Function-1 domain (A/B), followed by aDNA-Binding domain (C), the flexible hinge region (D) and the C-terminal ligand binding domain (LBD) (E/F). (B) The cartoon diagram of RORγt binded with coactivator shows all 14 helices and two **β**-sheets.

1.5 RORγt-related diseases

Th17 cells producing interleukin-17 (IL-17) require RORγt to fully differentiate from naïve CD4+ T cells. Interleukin-17 (IL-17) are responsible for amplifying inflammatory processes (Zenobia & Hajishengallis, 2015). Identifying these cells as critical mediators of autoimmune diseases has enabled the development of targeted therapies aimed at disrupting the activity of Th17 cells. Genetic ablation of RORγt alone or together with RORα has helped in preventing experimental autoimmune encephalomyelitis (EAE), a mouse model for multiple sclerosis (Parrado et al., 2001). This has caused a decline in Th17 cell differentiation. The data suggests that it might be possible to decrease autoimmune pathology by introducing some specific synthetic ligands inhibiting RORγt into mice. Over recent years, there has been much attention on RORγt since its absence precludes full maturation of this kind of lymphocytes (Rutz et al., 2016). Thus, pharmacologic repression of RORγt could provide an attractive starting point for developing new drugs against inflammatory diseases. Presently available immunosuppressants have serious adverse effects when used to treat Th17-mediated autoimmune diseases. Targeting RORγt is a significant advantage for the treatment of autoimmune disease.

According to recent studies, RORγt may have an impact on the development of tumors and the course of cancer. This nuclear receptor, traditionally studied for its roles in immune regulation and metabolism, is now being recognized for its involvement in tumorigenesis(Fan et al., 2018). Targeting RORγt pathways presents a promising possibility for cancer therapy, particularly in cancers where RORγt expression is altered

Studies have also demonstrated that RORγ expression varies significantly across different types of breast cancer. In estrogen receptor-negative (ER) breast cancer, RORγ levels are typically lower (Oh et al., 2016). Interestingly, higher levels of RORγt expression have been associated with better clinical outcomes in breast cancer patients.

1.6 Mechanism of ligand binding and conformational changes in RORγt

In RORγt, the role of agonist binding to orthosteric binding pocket is explored and it activates many downstream genes that result in complicated and unanticipated biological responses. But when an antagonist or inverse agonist binds at the same site it represseses the gene transcription. RORγt is a proven target for autoimmune disorders; its transcription function can easily be modulated by small molecules (called as modulators for RORγt). Once the modulator binds to the orthosteric binding pocket, it enables the protein-binding site to recruit either the co-activator or co-repressor . The conformation of H12 (also known as AF2, activation function 2) adopts a different conformation in response to binding of the different modulators at the orthosteric binding pocket. Binding of agonist and partial agonist at orthosteric binding pocket stabilizes the conformation of H12 at the LBD which is known to recruit a co-activator (steroid receptor activator 2 (SRC2)) at the protein binding site. While binding of antagonist and inverse agonist at the orthosteric binding pocket completely disables or reorients the H12 confirmation of LBD, by repressing the gene transcription function of RORγt. The mechanisms of these conformational changes resulting from ligand binding are still unclear, despite the fact that this structural information has profoundly illuminated about how RORγt binds with an agonist or inverse agonist and where H12 of the LBD may interact with or reorient relative to the surrounding structural components.

1.7 Mechanistic insights and therapeutic implications

The question arises: how does the binding of agonists and partial agonists in the ligand-binding pocket cause stabilization of H12? This further corresponds to the recruitment of the coactivator at the protein binding site. H12 destabilization results from binding of inverse agonist and antagonist which prevents the coactivator from binding to RORγt. It has been proposed that the binding of agonist and partial agonist or antagonist and inverse agonist can play a crucial role in the activation and deactivation of transcriptional activity of RORγt. Therefore, it is important to study and evaluate the mechanism that underlies these structural conformation changes. Such understanding of dynamic conformation changes that occur due to the binding of different modulators can be very helpful for the further designing of

novel RORγt modulators with better efficacy and pharmacodynamic properties that enhance cellular activity, alongwith potent inhibition of IL-17 release, and better oral bioavailability.

In our study, we have selected a system of RORγt without ligand (APO form; PDB ID: 5X8U) and two different systems that were bound with different modulators: agonist (6E3G), antagonist (8GXP), at orthosteric binding pocket. In our study, we will also be working on finding the structure determinants responsible for the stability of H12 in RORγt. Furthermore, we plan to perform molecular dynamic (MD) simulations on all three systems to monitor the intermolecular and intramolecular interaction.
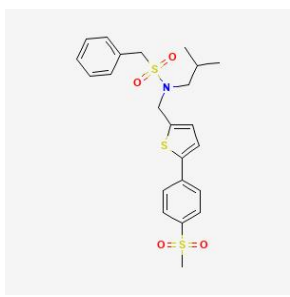
Additionally, we also hypothesize that the binding of agonist stabilizes H12 while when antagonists are bound to the orthosteric binding pocket of RORγt, the H12 orientation collapses. Due to the destabilization of H12, it would not be able to form the expected protein-binding site; further leading to the disruption of the transcription function of RORγt. To profoundly understand the orientation of H12, find the structure determinants responsible for stabilizing and destabilizing H12, we would be performing simulations. These insights into dynamic conformation changes and structure determinants, which are responsible for the binding of agonists andantagonists, will be crucial for developing greater potency and specificity modulators (agonists, and antagonists) that may be employed as a potential treatment of disease that is related to RORγt.
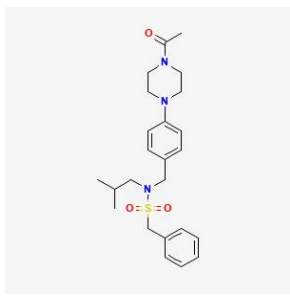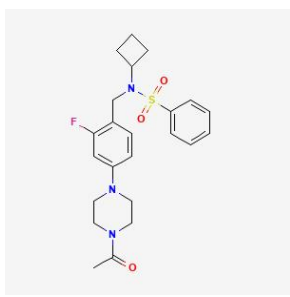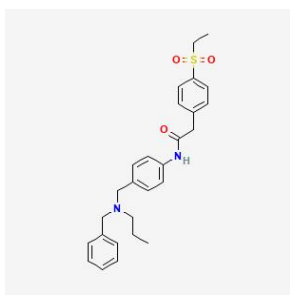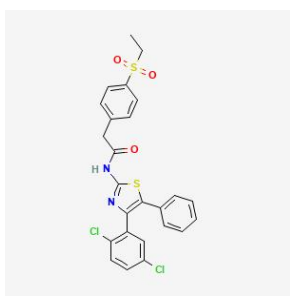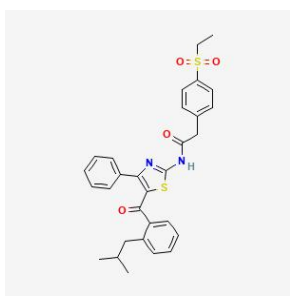
2. Materials and Methods
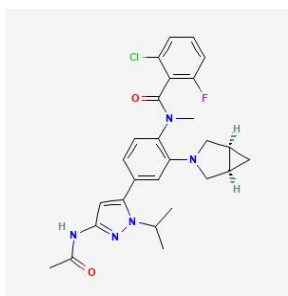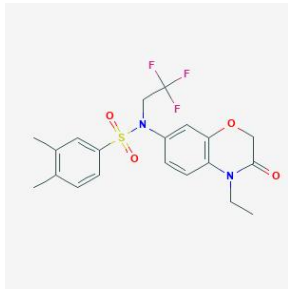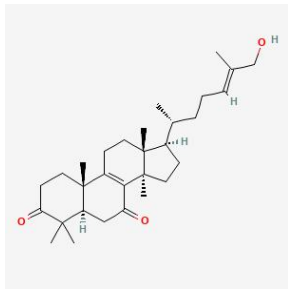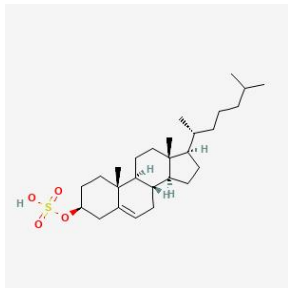
2.1 Mining of crystal structure
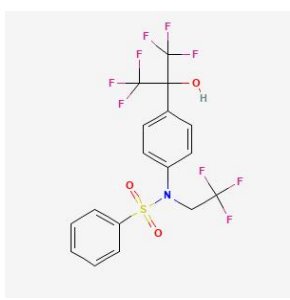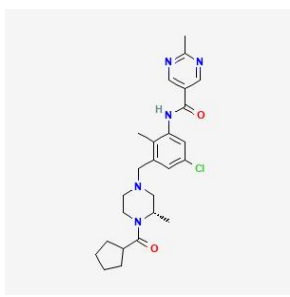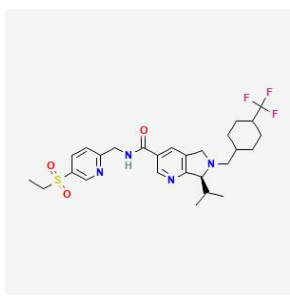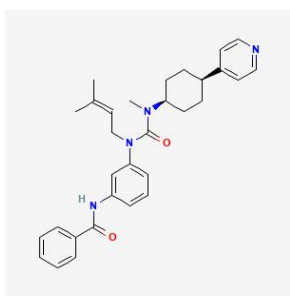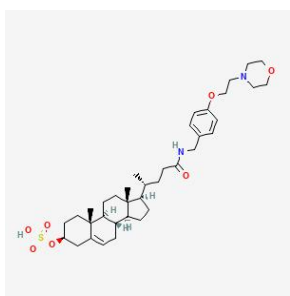
RORγt was first coined and described by (He et al., 1998) as an isotope of RORγ. RORγt is expressed mainly in CD4+ and CD8+ thymocytes. The protein crystal structure of RORγt is retrieved to study the effect of different modulators on the function of RORγt. In structural biology, protein crystal structures are the gold standard because they provide insight into the crucial interactions for various mechanisms of action (MOAs), which is essential for drug discovery. The structure of RORγt remained obscure for many years due to the absence of natural ligands for RORγt. We have searched various databases, including UniProt, PDB and the published literature in which work onRORγt structure is related. The keywords used for the search of crystal structure include RORγt, retinoid-related orphan receptor-gamma, RAR-related orphan receptor C, and RORC. From searching various databases and extensive literature scanning, we found 34 co-crystal structures of RORγt bound with different modulators like agonist, antagonist, partial agonist and inverse agonist (Tabel 1). We retrieved their coordinates from PDB (Berman et al., 2000). These co-crystals are bound with natural agonists, synthetic agonists, partial agonists, inverse agonists and antagonists. Most of the crystal structures are solved at good resolution (<2.5 °C). Interestingly, all the ligands that are found in co-crystals bind in the same pocket of
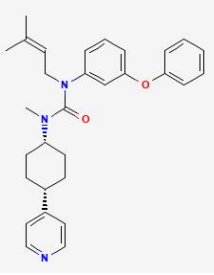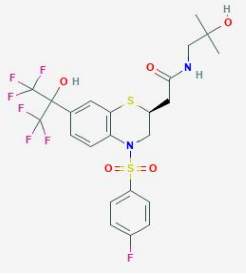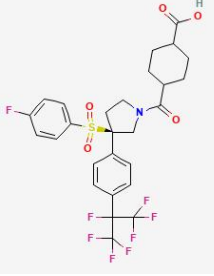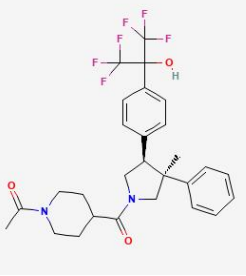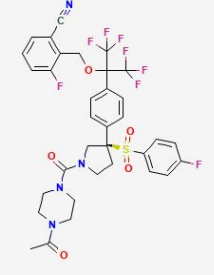
Tabel 1: Co-crystal structure of RORγt with different modulators
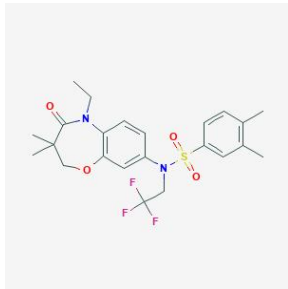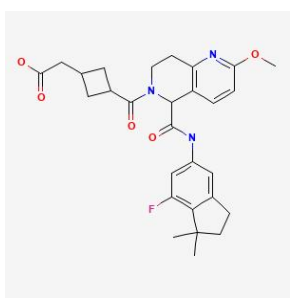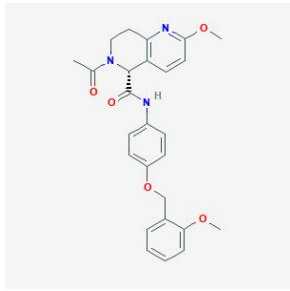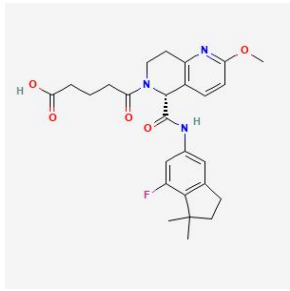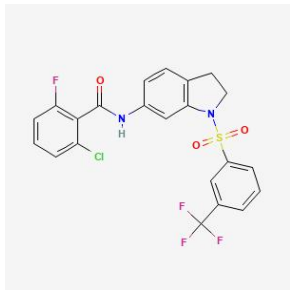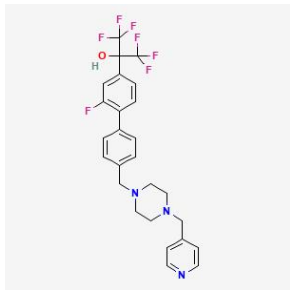
PDBs ID	Biological Activity	2D structure	Reference
4QM0	Inverse agonist		(Fauber et al., 2014)
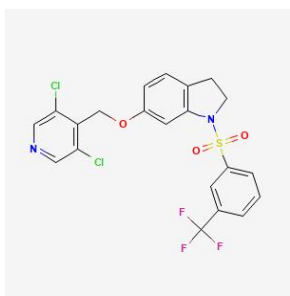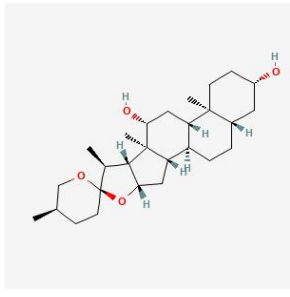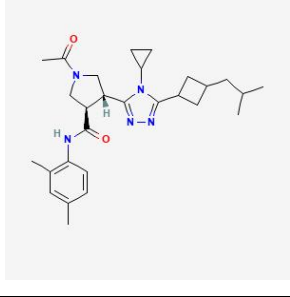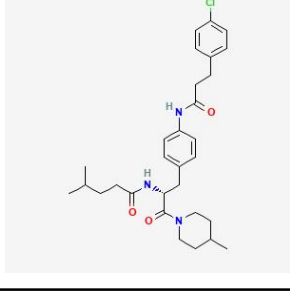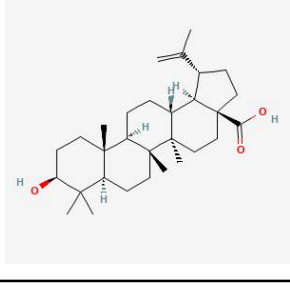
4WQP	Inverse agonist		(van Niel et al., 2014)
4WPF	Agonist		(van Niel et al., 2014)
4NIE	Inverse agonist		(Yang et al., 2014)
4XT9	Partial agonist		(Y. Wang et al., 2015)
5YP5	Agonist		(Y. Wang et al., 2018)

4ZOM	Inverse agonist		(T. Wang et al., 2015)
5IXK	Agonist		(Marcotte et al., 2016)
5IZ0	Inverse agonist		(Marcotte et al., 2016)
5NTN	Agonist		(Kallen et al., 2017)
5NTI	Agonist		(Kallen et al., 2017)

5NTQ	Agonist		(Kallen et al., 2017)
5NTP	Inverse agonist		(Kallen et al., 2017)
5NTW	Inverse agonist		(Kallen et al., 2017)
5VB6	Inverse agonist		(Li et al., 2017)
5NTK	Antagonist		(Kallen et al., 2017)

5VB7	Agonist		(Li et al., 2017)
6BN6	Inverse agonist		(Gong et al., 2018)
6P9F	Inverse agonist		(Lu et al., 2019)
6XFV	Inverse agonist		(Harikrishnan et al., 2020)
7JH2	Inverse agonist		(Shi et al., 2020)

6BR3	Inverse agonist		(Kono et al., 2018)
6E3G	Agonist		(Yukawa et al., 2019)
6E3E	Inverse agonist		(Yukawa et al., 2019)
6NWS	Agonist		(Strutzenberg et al., 2019)
6NWT	Agonist		(Strutzenberg et al., 2019)

6NWU	Agonist		(Strutzenberg et al., 2019)
5X8Q	Inverse agonist		(Noguchi et al., 2017)
5X8X	Inverse agonist		(Noguchi et al., 2017)
5VB5	Inverse agonist		(Li et al., 2017)
8GXP	Antagonist		(Mei et al., 2023)

Table 2: Apo crystal structure of RORγt

5X8U (Co-activator)	—		(Noguchi et al., 2017)
5X8W (Co-activator)	—		(Noguchi et al., 2017)
5VB3 (Co-activator)	—		(Li et al., 2017)

the RORγt, which is the orthosteric binding pocket . From these 34 co-crystal structures We take each crystal structure of agonist, antagonist, partial agonist and inverse agonist to study the mechanism of action (MOAs) of these modulators on RORγt and conformational change, which are essential for the regulation of biological activity of RORγt.

2.1 Preparation of crystal structure of RORγt using protein preparation wizard

The Protein Preparation Wizard developed by Schrödinger is a valuable tool for ensuring the structural accuracy of proteins at the beginning of a project (Lu et al., 2019). It offers researchers a reliable and high-confidence protein structure that is well-suited for various modeling applications. Going beyond simple structural corrections, the Protein Preparation Wizard combines and automates commonly used tools and techniques in structure preparation. This comprehensive approach ensures a solid starting point for structure-based projects, making it an appealing choice for researchers who depend on precise protein models.

To prepare the protein structures RORγt, the details of all systems are described in Table 2. employed the Protein Preparation Wizard utility available in Maestro. First, protein hydrogens were added while considering stereochemistry. The appropriate ionization states of acidic and basic amino acid residues were maintained at pH 7.0. Missing side-chain atoms were then added using the rotamer library developed by Xiang and Honig. Subsequently, structure optimization was performed, focusing on maximizing hydrogen bonding. This optimization process involved identifying the most probable positions for freely rotating hydrogens (-OH and -SH), assigning correct protonation states to charged

residues, determining tautomers of His residues, and considering Chi 'flip' for Asn, Gln, and His residues. Finally, the structures were subjected to energy minimization using the OPLS4 force field to alleviate any steric clashes between atoms. The energy minimization continued until the heavy-storm displacement reached a root mean square deviation (RMSD) of 0.30 Å.

Table 3. The details of the RORγt complexes for Protein Preparation

PDB ID/Chain	Ligand Bounded	Coactivator
5X8U	No-ligand Bound	SRC2
6E3G	Agonist	SRC2
8GXP	Antagonist	SRC2
5NTW	Inverse Agonist	SRC2
4XT9	Partial agonist	SRC2

2.2 Identification of all possible ligand binding sites using SiteMap for RORγt protein

Understanding the structure and exploiting the function of protein active sites is essential for drug design projects and protein-ligand interaction studies. However, at the beginning of many drug design projects, the location of binding sites for protein-ligand or protein-protein interactions is often unknown. Additionally, identifying potential allosteric binding sites is equally important. SiteMap is a widely used algorithm for binding site identification and evaluation, known for its effectiveness in locating binding sites with high confidence and predicting their druggability.

In the case of the protein, we utilized SiteMap to identify possible interaction sites. By analyzing the RORγt protein's PDB structure, SiteMap provided valuable information about potential sites where ligands could interact with RORγt to exert negative regulation or positive regulation of RORγt.

2.3 Molecular docking

In our study, we employed AutoDock4 (Bitencourt-Ferreira et al., 2019) to perform protein-ligand docking between RORγt and their different modulator.

2.3.1 AutoDock4

AutoDock4 is a widely used tool for docking small molecules to macromolecules, using a physics-inspired scoring function which is beneficial in drug discovery studies. It uses a semi-empirical force field to evaluate the protein-ligand interaction binding affinity, and it uses various search algorithms like simulated annealing and genetic algorithms for docking simulation. Additionally, the studies have explored the impact of the number of runs on the validity of docking results with AutoDock 4. We employed AutoDock 4 for blind docking and focused docking.

Blind Docking

Blind docking studies were performed through AutoDock4 by using the Lamarckian genetic algorithm. The prepared Holo protein structure RORγt from PDB id 6E3G and 8GXPwere used as receptors for the blind docking study of ligands Agonist, Antagonist, Partial agonist, and Inverse agonist. Grid maps were generated for the entire protein with 0.375 Å spacing using Autogrid 4. Docking was performed by using the search parameter genetic algorithm (GA) with 200 GA runs, and other parameters are default. The best binding poses were chosen from the top cluster based on the highest docking score.

Focused Docked

Focused docking was performed using AutoDock4 by utilizing the Lamarckian genetic algorithm (LGA). The grid box was taken as the center of the ligand, with a spacing of 0.375. Docking was performed by using the search parameter genetic algorithm (GA) with 200 GA runs, and other parameters are default. The best binding pose was chosen from the top cluster based on the highest docking score.

By utilizing these docking tools, we aimed to explore the other docking site or find a potential binding site other than the crystal structure between RORγt and their different modulators.

Based on cluster size and binding energies, we have chosen a site where we perform focused docking

Induced fit Docking

IFD is an advanced docking protocol that considers the receptor flexibility besides ligand flexibility. Though the rigid docking classically considers the receptor as a rigid, another induced fit docking protocol with the receptor treated in such a way that during the docking of a ligand, it is allowed to have a conformational change. This is premised on the fact that the original biological molecules do not form rigid structures but can attain a conformation appropriate for ligand binding.

2.4 Prime MM-GBSA

The binding free energy of all three protein-peptide complexes was carried out in prime MM-GBSA (molecular Mechanics Generalized Born Surface Area) (Kumari et al., 2022). The binding free energies of the protein-peptide complex were calculated using the Prime MM-GBSA module of the Schrodinger Suite with an OPLS4 force field. The binding free energy of a peptide to a protein (P) to form the complex (PL) is obtained as the difference.

$$\Delta G_{binding} = \Delta G_{(complex)} - \Delta G_{(Protein)} - \Delta P_{(peptide)} \qquad (1)$$

Where $\Delta G_{binding}$ is the binding free energy; whereas $\Delta G_{complex}$, $\Delta G_{protein}$ and ΔG_{ligand} represent the free energy of complex, protein, and peptide, respectively.

2.5 Molecular Dynamics Simulation

Molecular dynamics (MD) is a scientific approach used to simulate the motions of particles within a system. It can be applied to various systems, from individual atoms and molecules undergoing chemical reactions to large-scale structures like galaxies. In MD simulations, the interaction potential between particles is crucial for calculating the forces acting on them. By simulating particle motions over time, MD allows for detailed investigations into the properties of a system, offering insights that are difficult to obtain through experiments alone. The user has control over the simulation potential, enabling the examination of specific contributions to understand their role in determining system properties. Additionally, the technique of computer alchemy allows for the manipulation of potentials during a simulation, enabling the calculation of free energy differences.

To initiate a dynamic simulation, initial atomic coordinates and velocities are required. These coordinates can be obtained from experimental techniques like X-ray crystallography or NMR, or through model-building techniques based on the structure of a related protein. The system is then equilibrated through a series of steps. Firstly, a refinement process involves iterative minimization to relieve local stresses, such as atom overlaps and bond length distortions. Next, velocities are assigned to atoms based on a Maxwellian distribution at a low temperature, and a short simulation is performed. The widely used Verlet algorithm is often employed for these simulations.

MD simulations typically involve three stages: data preparation, production simulation, and result analysis. There are several software packages available for MD simulations, including GROMACS, NAMD, AMBER, Desmond, Yasara, Hypercube Hyperchem, Spartan, and Chemoffice, among others.

In our study, we utilized the AMBER software for simulating the interaction between the RORγt receptor protein and their different modulators. The MD simulations in AMBER involve several steps. Initially, the coordinates are loaded in PDB format along with the chosen force field. Subsequent steps include adding ions, setting periodic boundary conditions, adding solvent, performing energy minimization, and equilibration. The production MD run is then executed. We employed the AMBER22 software package for conducting extensive MD simulations of the complex systems.

The protein systems were prepared for simulation using the LEaP software within the AMBER package. The AMBERff14SB force field (Kumari et al., 2023) was applied to the proteins, and hydrogen atoms were added. and counterions were included to neutralize the systems. Periodic box conditions were established by filing a cubic box of dimensions 12.0 Å with atomistic TIP3P water molecules surrounding the protein. The system underwent a three-phase minimization process to relax the structure, remove steric hindrances, and correct any faulty connections. The systems were minimized over 2000 steps using the steepest descent approach followed by 1000 steps using the conjugate gradient technique. Solvent molecules were relaxed through two stages, with position restraints of 10 and 2 kcal/mol/Å^2 applied to the entire protein system. The third stage involved unrestrained relaxation.

Table 4. Summary of the RORγt complexes for MD simulation

System	MD length (ns)	Solute atoms	ions	Water molecules	Total atoms

Apo - coactivator (system A)	300	4175	3	37680	41858
COM - A (system B)	300	4235	4	39831	44070
COM - ANTA (system C)	300	4331	5	40560	44896

Subsequently, the systems were gradually heated from 0 to 300 K over 20 ps, followed by density equilibration for 50 ps. The systems were further equilibrated at 300 K and 1 atm pressure for 500 ps. Molecular systems were then subjected to simulations of 300ns, with a time step of 2.0 ps. Coordinates were recorded every 20 ps, resulting in a total of 15,000 frames, using various seed values.

2.6 Calculation of Binding Free Energy using MM-PBSA in AMBER22

The calculation of binding free energy (ΔG) for our complexes was carried out using the MM-PBSA method implemented in Amber22 (Kumari et al., 2023). MM-PBSA is a computational approach that determines the free energy difference between two states, typically representing the bound and unbound states of solvated molecules or different conformations of the same molecule. In our study, we aimed to accurately estimate the average ΔG by extracting 100 snapshots at regular intervals from the stable region of the equilibrated molecular dynamic (MD) trajectory.

The ΔG value was calculated by combining the vacuum potential energy, which accounts for both bonded and nonbonded interactions, with the free energy of solvation, taking into consideration both nonpolar contributions. area (SASA) approach was employed. On the other hand, the nonpolar solvation energy term was polar estimated using the Poisson-Boltzmann equation. To evaluate the contribution of each residue in the complex formation to the overall ΔG, the Poisson-Boltzmann (PB) model was

protein-peptide utilized. The same number of frames was used for this analysis across all complexes. For the polar solvation energy term, the solvent-accessible surface

The binding free energy (ΔG_{bind}) on each system is evaluated as follows:

$$\Delta G_{bind} = G_{com} - (G_{rec} + G_{lig}) \tag{1}$$

where Gcom, Grec, and Glig are the absolute free energies of complex, receptor, and peptide respectively, arranged over the equilibrium trajectory. The free energy, G, for each species, can be calculated by using MM-GBSAand MM-PBSA approaches as follows:

$$G = Egas + Gsol - TS \tag{2}$$

$$Egas = Eint + Eele + Evdw \tag{3}$$

$$Gpolar,PB(GB) = Eele + Gsol - polar,PB(GB) \tag{4}$$

$$Gnon-polar,PB(GB) = Evdw + Gsol - np,PB(GB) \tag{5}$$

$$Gsol = GPB(GB) + Gsol - np \tag{6}$$

$$Gsol -np = \gamma SAS \tag{7}$$

where S and T stand for the total solute entropy and temperature, respectively. The total of the internal energy (Eint), van der Waals interaction energy (Evdw), and electrostatic interaction energy (Eele) is called the gas phase energy (Egas). The AMBERff12SB force field's parameters are used to calculate it.The solvation-free energy, or Gsol, is divided into polar and non-polar components. The polar solvation contribution, Gsol-polar, GB, is determined by solving the Poisson-Boltzmann (PB) and Generalized-Boltzmann (GB) equations.The sum of the Eele and (Gsol-polar, PB(GB)) was used to

determine the total polar interaction contributions (Gpolar, GB). The non-polar solvation contribution, denoted as Gsol-np, was calculated by measuring the solvent-accessible surface area (SAS) with a water probe radius of 1.4 Å and utilizing 0.0072 kcal mol-1 Å-2 (value of constant γ). Solute and solvent dielectric constants were set to 1 and 80, respectively. Evdw and Gsol-np, GB were used to calculate the total non-polar interaction contributions (Gnon-polar, GB). Using the same number of frames and the GB model, the binding free energy contribution for each residue in the formation of the protein-ligand complex was calculated.

2.7 Post-MD analysis

To assess the overall stability of the system, we conduct several analyses including root mean square deviations (RMSDs) of backbone atoms, root mean square fluctuations (RMSFs), the radius of gyration (RG), and solvent accessible surface area (SASA). These analysis were performed using VMD.

2.8 Visualization and Analysis Tools: VMD and PyMOL

PyMOL and VMD were used throughout the project to accomplish a variety of visualization tasks, including Post MD analysis, selecting docking poses, rendering various structures, and changing the colours of molecules, atoms, and chains.

2.8.1 Visual Molecular Dynamics (VMD)

Visual Molecular Dynamics (VMD) (Humphrey et al., 1996) was employed for the analysis and animation of molecular dynamics (MD) simulation trajectories. VMD offers a wide range of methods for rendering and colouring molecules, including points, lines, spheres, cylinders, bonds, tubes, ribbons, and cartoons. It can serve as a graphical interface for displaying and animating molecules undergoing simulation on remote computers. VMD's Key features include support for many molecules, atoms, residues, and trajectory frames, extensive atom selection syntax for flexible subset display, compatibility

with various molecular file formats, and integration with bioinformatics analysis tools for sequence and structure data. VMD also allows exporting graphics to files that can be further processed by ray tracing and image rendering packages. It offers user-extensible graphical and text-based interfaces using Tcl/Tk and Python scripting languages.

2.8.2 PyMOL

PyMOL, which stands for Python Molecular Graphics, was created by Warren Lyford DeLano as an open-source molecular visualization system . Schrödinger, Inc. now commercializes this software. PyMOL is widely recognized for its ability to generate high-quality 3D images of diverse molecular structures, ranging from small molecules to complex biological macromolecules like proteins. Notably, it is one of the primary open-source tools available for visualizing molecular structures in the field of structural biology. The name "PyMOL" is derived from the fact that the software is primarily written in the Python programming language.

2.9 Data Plotting and Refinement using Xmgrace

Xmgrace is a widely used plotting package available for the Linux operating system. It offers various features to enhance the descriptive quality and comprehensibility of graphs. Among the tools available for graphing data, xmgrace stands out for its versatility and ability to generate high-quality graphical images.

In our study, Amber produced graphs in either 'dat' or 'agr' format. These graph files were opened in xmgrace for further editing and refinement. Xmgrace allowed us to fine-tune the plot-data sets, adjust plot-axes properties, and add plot titles and legends. Additionally, we utilized xmgrace to save the graphs as high-quality images in PNG format.

2.10 Analysis of Protein-Ligand Interactions using PDBsum

To analyze the interactions between the residues RORγt and their modulators, we utilized the PDBsum database. PDBsum provides a visual database that offers a quick overview of the contents of each 3D structure deposited in the Protein Data Bank. It displays the molecules involved in the structure, such as

protein chains, DNA, ligands, and metal ions, and presents schematic diagrams of their interactions. To visualize the molecules and their interactions in 3D, we made use of the RasMol, JSmol, and PyMOL molecular graphics programs, which are freely available.

For our analysis, we examined the representative complex structures. This allowed us to gain insights into the protein-ligand interfaces and the interactions between specific residues across these complexes.

3. RESULT

3.1 RORγt: LBD Structure and Ligand Binding Site Analysis

The arrangements of the crystals in RORγt + co-activator (system A), RORγt + co-activator +agonist (system B), and RORγt + co-activator+antagonist (system C) have indicated that the binding of agonist, and antagonist, at the RORγt-LBD pocket involves a conformational adaptation. Significant structural changes were observed upon a comparison between the bound and unbound forms (Fig 2).
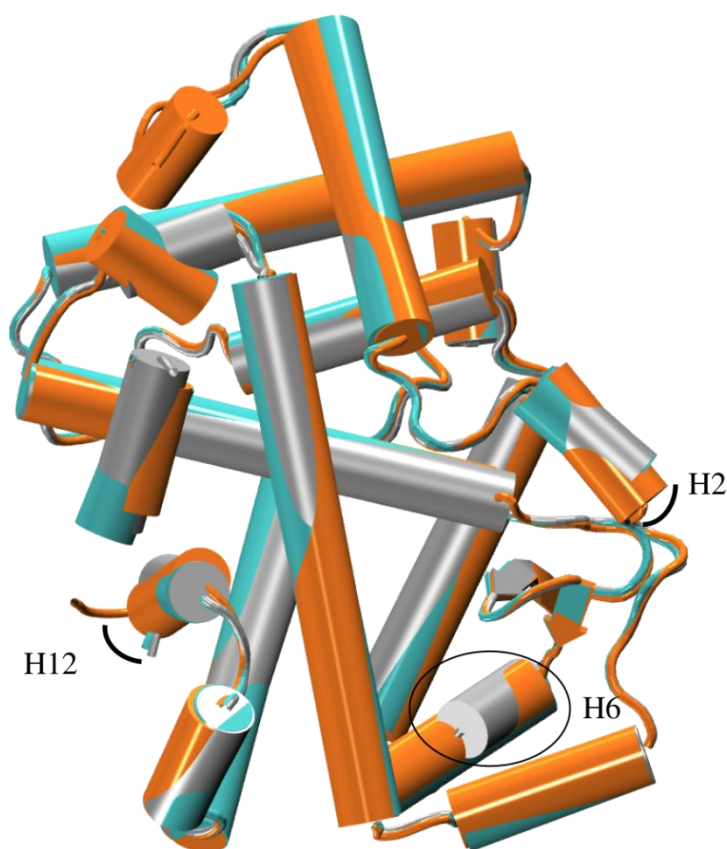
Fig 2: overall structure comparison of the different RORγt complexes. The structural comparison between system A (in silver), system B (cyan) and system C (in orange).

Concerning system C, the structure difference was observed in helices H2, H11, H11', and H12. These structural changes due to concerted movement induced by ligand binding are essential to explore, particularly between agonists, and antagonists

At the ligand binding site of RORγt, the following residues are involved: Cys285, Gln286, Leu287, Leu292, Trp317, Cys320, Ala321, His323, Leu324, Ala327, Met358, Val361, Arg364, Met365, Val376, Arg367, Ala368, Phe377, Phe378, Glu379, Leu391, Cys393, Leu396, Ile397, Ile400, Trp401, Arg482, Tyr502. Around 80% of the ligand-binding pocket is composed of non-polar amino acids, which are Phe (phenylalanine), Trp (tryptophan), Met (methionine), Ala (alanine), Val (valine), Ile (isoleucine), and Tyr (tyrosine), which contribute to the formation of non-covalent interactions Ligands typically interact non-covalently and reversibly with proteins to form bonds.
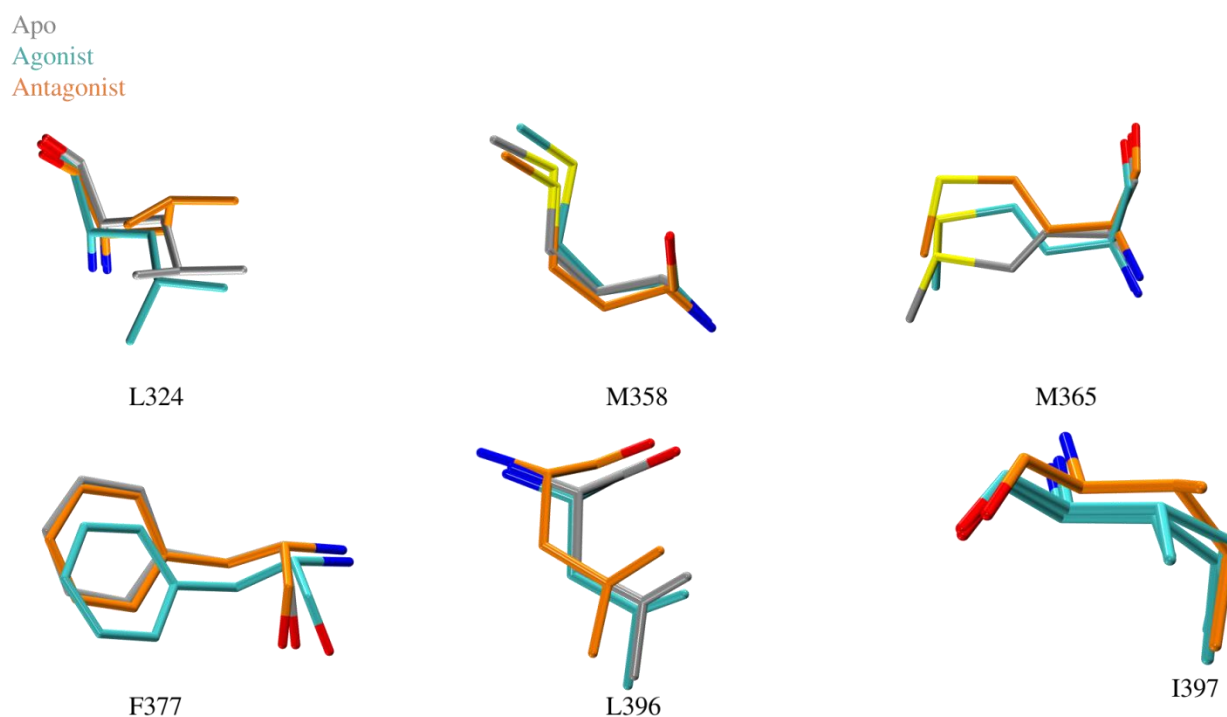
Fig 3: The superimposition of the ligand pocket residue which shows conformational changes in the complex of Apo (silver), agonist (cyan), and antagonist (orange) .

Furthermore, a comparative analysis of ligand-binding pockets between all systems was performed. It was observed that the agonist was intact closer to helix H5 and loop L: H1/H2, while the antagonist was

intact closer to helix H11' and H12 in terms of major structural changes. However, these complexes largely share the same residues in the binding site.

When superimposing the binding pocket of all complexes, we observed outward movement of L324 upon binding of antagonists with RORγt, while inward movement was observed upon binding of agonists. Furthermore, we observed side chain movement in binding pocket residues L324, M358, M365, F377, L396, and I397 in these complexes (Fig 6).

Crystallographic study shows that binding of the agonist and antagonist causes significant conformational changes in RORγt, which may control the different mechanisms of action.

3.2 **Search for Binding Sites Other than Crystal Binding Site**

Why do we need to perform binding site identification when we already have a crystal structure?
For the purpose of finding every possible potential binding site of RORγt as well as confirming that the co-crystal site is the primary binding site, we performed binding site identification. We performed ligand-independent binding site searches on RORγt to explore all the possible sites where ligands bind to proteins or identify any binding site other than the co-crystal binding site.

By reviewing the published literature, we were able to identify ligand binding sites (LBD)and allosteric binding sites. To confirm these sites and check the robustness of the SiteMap programme of Maestro as well, we performed a SiteMap analysis for RORγt.

The top score of the SiteMap programme confirmed that the co-crystal site is the primary binding site (marked as site 1), with the highest DScore of 1.259 (the best druggability score). The volume of the pocket was 393.078 Å3, solvent exposure was 0.354, and SiteScore was 1.199. But we also found four pockets other than the co-crystal site (marked as sites 2 to 5) (Fig 4). The D scores of other sites from 2 to 5 were 0.938, 0.782, 0.746, and 0.458, respectively. The volumes of these pockets were 395.136, 160.181, 110.466,and 37.730,respectively. From the SiteMap results, we deduce that RORγt might have other binding sites as well, which are different from the previously reported co-crystal binding sites.

Also, site 2 identified by the SiteMap has previously been reported as an allosteric site in the literature, whose volume size is larger than the binding site (co-crystal site).
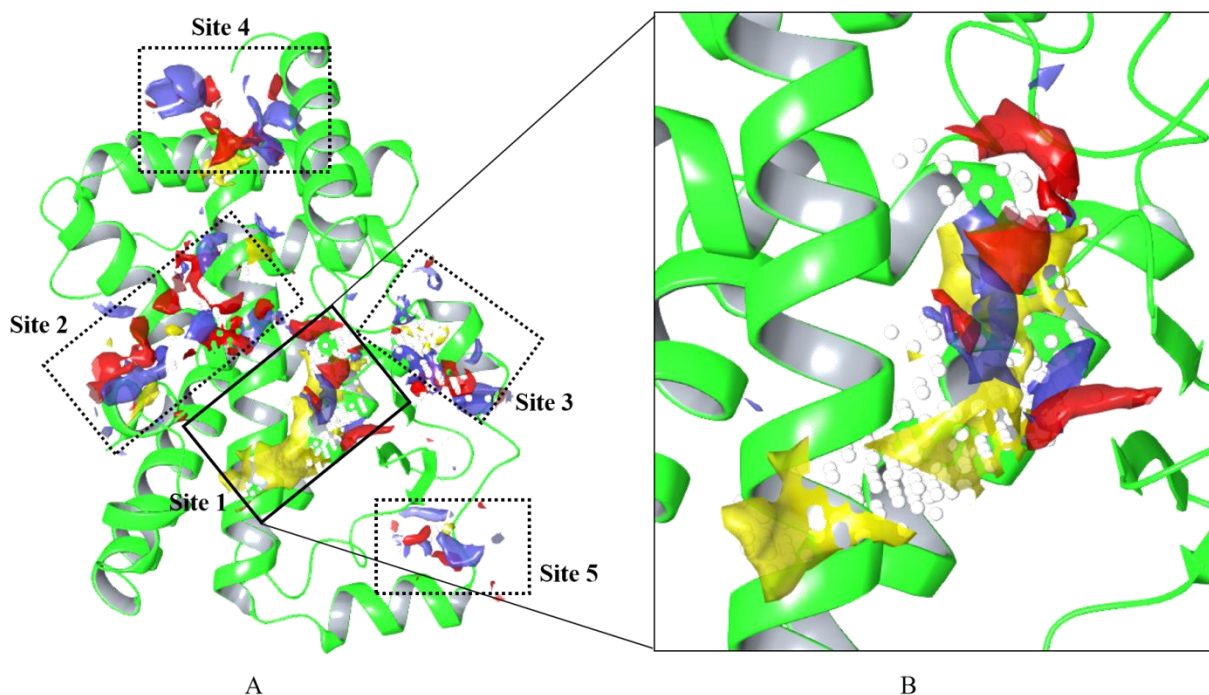
Fig. 4. Site Map Binding site Prediction: The potential binding sites identified by SiteMap. The yellow, red and blue regions show the hydrophobic, ligand acceptor and ligand donor sites, respectively. (A) The sites that have been identified are shown in dotted boxes. (B) SiteMap indicates the co-crystal binding site; zoom-in view.

Using Autodock 4, we perform blind docking on the crystal structures of RORγt. Blind docking is implemented to perform unbiased searching of possible binding sites. Using blind docking, we identified three distinct binding sites for agonist, antagonist, inverse agonist, and partial agonist (Fig. 5). Similar to the SiteMap result, ligands are docked at the same binding site in blind docking as well.

We perform blind docking with the ligands Agonist, and Antagonist from their respective co-crystal structures of RORγt (6E3G, and 8GXP) A blind docking does not require a ligand-binding site to be known before the docking, which creates more chances to find alternative binding sites not discovered by the co-crystal.

The binding result revealed that most ligands are docked at three different sites of the structure (shown in Fig 3): 6E3G, and 8GXP. In 6E3G, a total of 66 distinct conformational clusters were found, with the lowest binding energy being -10.86 Kcal/mol. Out of all these 66 different clusters, the top cluster size is 70, and its binding energy is -10.86 Kcal/mol. To analyze all clusters generated we take the cutoff value of binding energy as 7.0 Kcal/mol. One more cluster, which has a cluster size of 17, is found on different sites, and its binding energy is -7.80 Kcal/mol. Further prime MM GBSA is performed to confirm the best binding of the two other sites found. The MMGBSA (ΔG) values of these two poses are -96.24 kcal/mol and -25.02 kcal/mol, respectively. A similar analysis is performed for the 8GXP also.

Table 5. Summary of the RORγt Bind docking and MMGBSA

PDB id	Site	Binding energy (Kcal/mol)	Number of clusters	MM GBSA (ΔG) (kcal/mol)
6E3G (Agonist)	Site 1	-10.86	70	-96.24
	Site 2	-7.80	17	-25.02
8GXP	Site 1	-13.20	162	-73.13
	Site 2	-8.38	17	-20.76
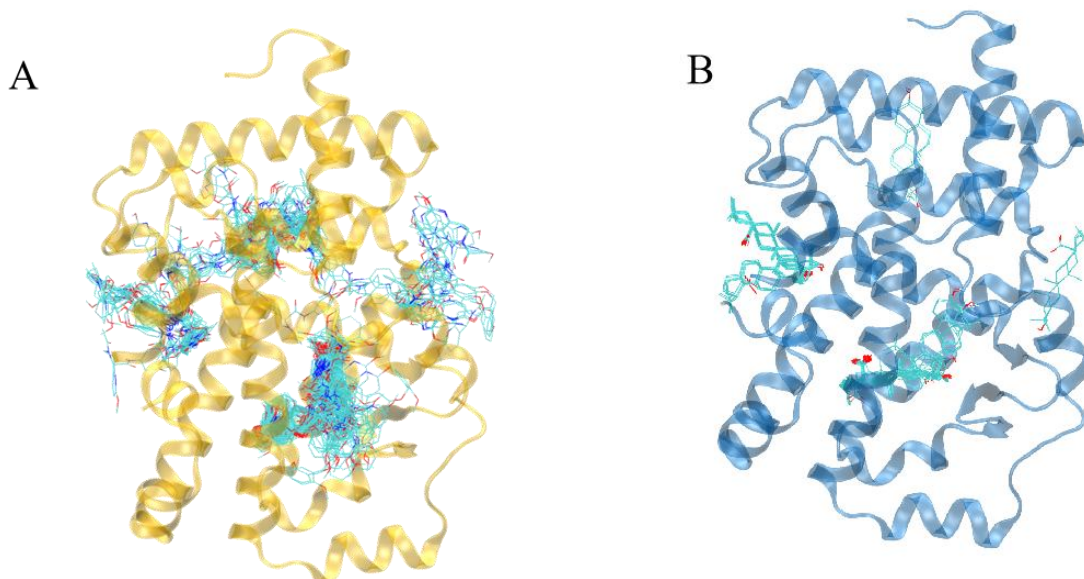
Fig. 5. Binding site Analysis: (A) All 200 poses of Agonist are shown in line and coloured atom-wise:C: cyan, N: blue, and O: red. Protein (6E3G) is rendered in cartoon form (in orange). (B) All 200 poses of

the antagonist are shown in line and coloured atom-wise: C: cyan, N: blue, and O: red. Protein (8GXP) is rendered in the cartoon (in blue).

In blind docking, there is no similar ligand pose found as a co-crystal pose. With the ligand pose having the lowest binding energy, MM GBSA($\triangle$G) value, and highest number of clusters, we further performed focused docking on that ligand binding site.

3.3 **Molecular Docking Studies**

The primary purpose of molecular docking analysis is to determine the interaction between a protein and a ligand. A binding site describes the interaction between a protein and ligand molecule, with the lowest binding energy representing the most significant interaction.

In our study, focused docking was performed at site 1 of RORγt structures to bring robustness to the final binding site. The cluster representative of agonists has a binding energy of -11.33, and antagonists have a binding energy of -13.42. The superimposition of the agonist and antagonist docked pose with their co-crystal pose has revealed that the obtained pose was close to the co-crystal pose, within the minimum RMSD deviation.

Furthermore, we perform docking of antagonist and Agonist bound protein (6E3G) to elucidate the residue which are responsible for binding of agonist and antagonist in different positions at the same pocket of RORγt protein. we perform rigid focused docking at the Agonist binding site. The lowest binding score -8.05 with cluster size 192. After analyzing we found that antagonists do not achieve the crystal binding pose (shown in fig 6). All the conformations bind similar position of agonist which means it doesn't goes deep inside the binding pocket.
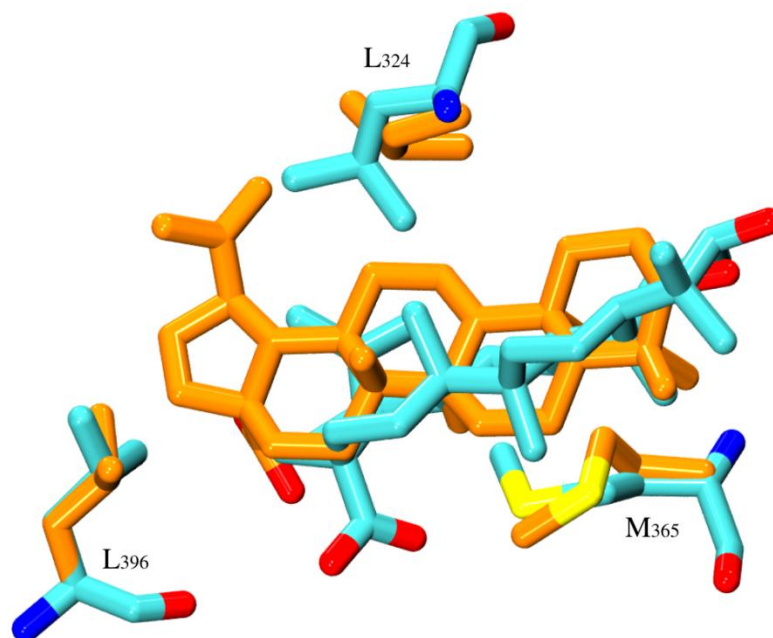
Fig 6: Binding pose of antagonist in Rigid Docking and residue shown in Licorice (cyan). The binding poses of the antagonist in Induced fit docking and residue which are flexible are shown in Licorice (orange).

Further we implement induced fit docking to check whether we achieve the crystal binding pose of the antagonist or not in Agonist bound protein. Residue which are in different conformation in agonist and antagonist bounded protein (shown in Fig 3). We make residue L324, M365, L396 as flexible for induced fit docking. The induced fit docking results are interesting: antagonists achieve the crystal pose having binding score -12.30 with cluster size of 164 (shown in Fig 6) and the residue L324 shows the maximum conformation changes. The induced fit docking revealed that the binding of agonist and antagonist majorly depend on conformation of L324. Thermodynamic analysis also shows that L324 in agonists showed higher binding affinity than antagonists (shown in Fig 24, 25).

3.4 **The Dynamical Exploration of RORγt in Three Different Systems.**

A molecular dynamics simulation was employed to govern the dynamic stability of the complex. To understand the conformational changes and dynamic stability of each complex the trajectory data file for the analysis were collected over the 300ns of the simulation period. Each system's time-dependent RMSD (root mean square deviation) was calculated, and the root mean square fluctuation (RMSF) was calculated for stability and fluctuations. Each complex was compared with its APO, with agonist, and antagonist. By analyzing the radius of gyration (Rg), we determined the compactness of the protein-ligand complex, indicating its folded and unfolded state. solvent accessible surface area (SASA) calculated the solvent accessible surface analysis was done using trajectory.

3.5 **Agonist Crystal vs Dynamic Insights.**

To elucidate the dynamic behavior of agonists on the RORγt we perform MD simulation of 300ns. The crystal pose gives a single frame of ligand binding which may change during time intervals to find the behavior of ligands on RORγt protein, MD simulation gives a good idea about that. As compared to the crystal pose and MD stable pose the binding site residues are almost the same but some residues are unique in the crystal pose and MD stable pose. The residues that were unique in crystal pose are GLN 286, L362 and LEU287 (shown in fig 7). PHE377 form Hydrogen with agonist crystal pose. In the MD pose these two residues are not in the binding site because of the movement of ligand in the binding pocket ARG482 in the binding site of the MD pose which lies in Helix H11'. in MD stable pose hydrogen bond forming residue are PHE377 and GLU379.
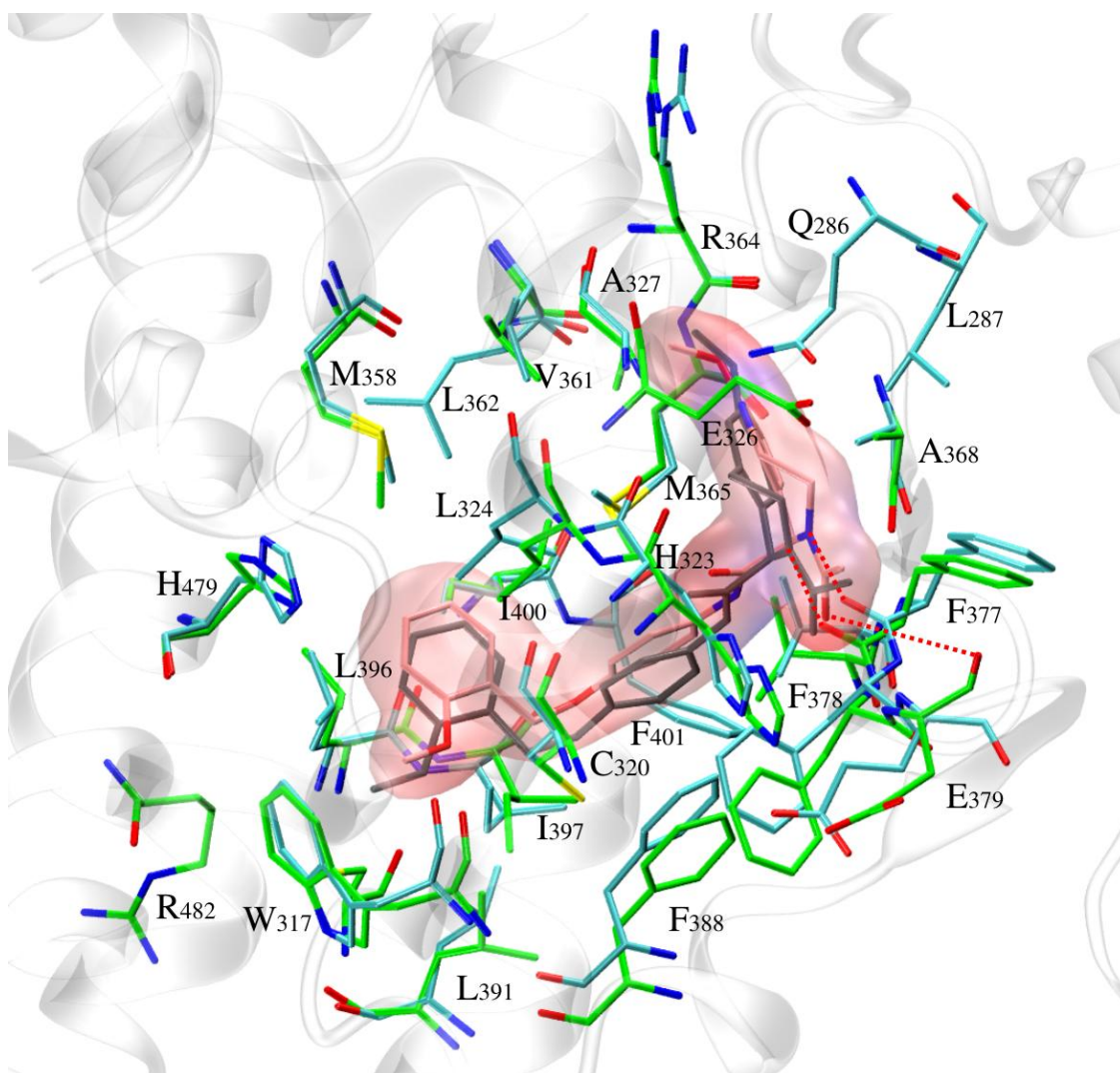
Fig 7: The superimposition of crystal structure binding site residues (cyan)and MD stable pose (green) indicated that most of the interacting residues have similar conformation. Ligandsof crystal structure (pink) and MD stable pose (gray) are shown in licorice. The HBonds are denoted dashed Lines (Red).

The dynamic stability of the Agonist bounded RORγt and Apo was compared to evaluate the dynamic behaviors of RORγt in Apo (without ligand bounded) and agonist bounded RORγt (Fig 8 A). The RMSD of protein of Apo shows an upward trend in the initial 20ns that gets stabilized throughout the simulation. The average RMSD value was 1.488. While in agonist bounded RORγt protein the RMSD plot showed that it shows initial 30ns upward trend then it forms a plateau till 250 ns and then a sudden shift of confirmation. This sudden deviation may occur due to the movement of the loop between Helix 1 and 2. The average RMSD value is 1.36.

To elucidate the binding site of RORγt protein after binding with Agonist we calculate the RMSD of binding site of Apo and Agonist bounded RORγt protein (Fig 8 B).
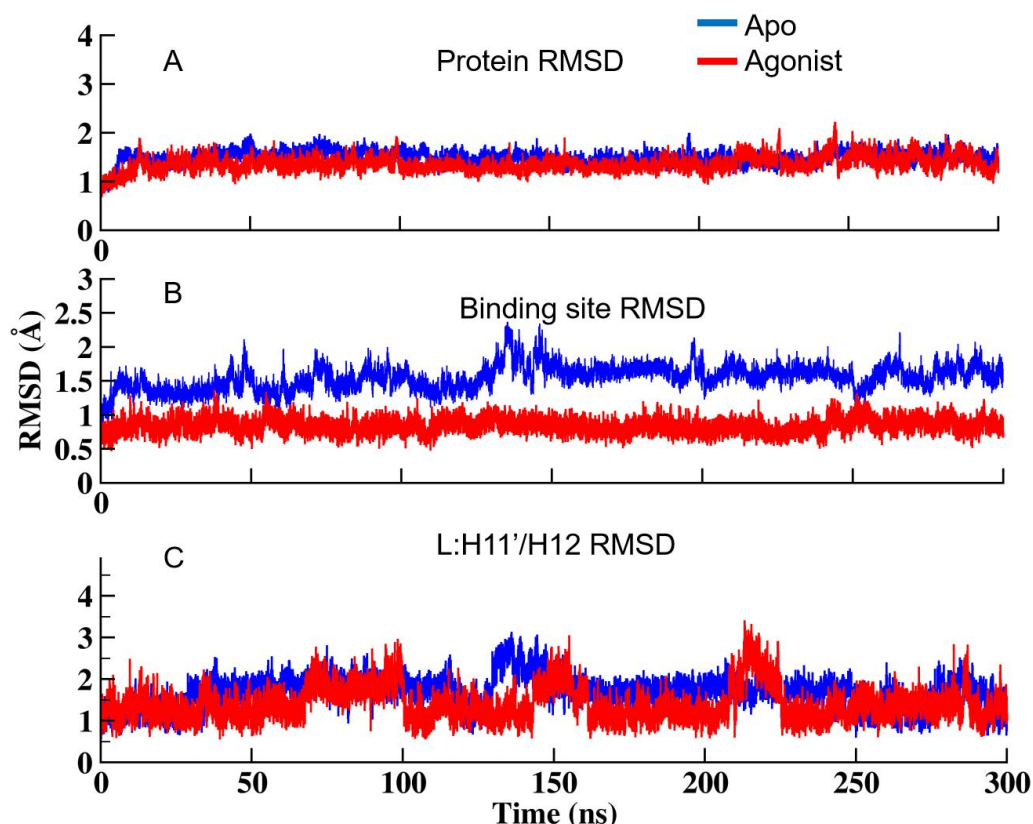
Fig 8: Through molecular dynamics simulations monitoring of time dependent dynamics changes. The RMSD was compared between Apo+coactivator and Protein+Agonist

The binding site RMSD plot shows that after binding to the agonist RORγt protein the binding site gets more stable than the Apo form. In Apo, the binding was more flexible due to open (or not bound to any ligand). The average RMSD values of the binding site of Apo and agonist-bounded Complex are 1.545 and 0.815 respectively.

Furthermore, we also calculate the RMSD of L: H11'/H12 (Fig 7 C) because L: H11'/H12 are involved in the activation of protein and previous studies show that the after-binding to agonist L: H11/H12 are stabilized. RMSD Graph of the apo shows that L: H11'/H12 was stable throughout the simulation within

the minimum fluctuation due to the C-terminal region (Fig 9). In the Agonist bounded complex the RMSD plot shows that L: H11'/H12 was more stable than Apo and some fluctuations were seen due to the C-terminal region.
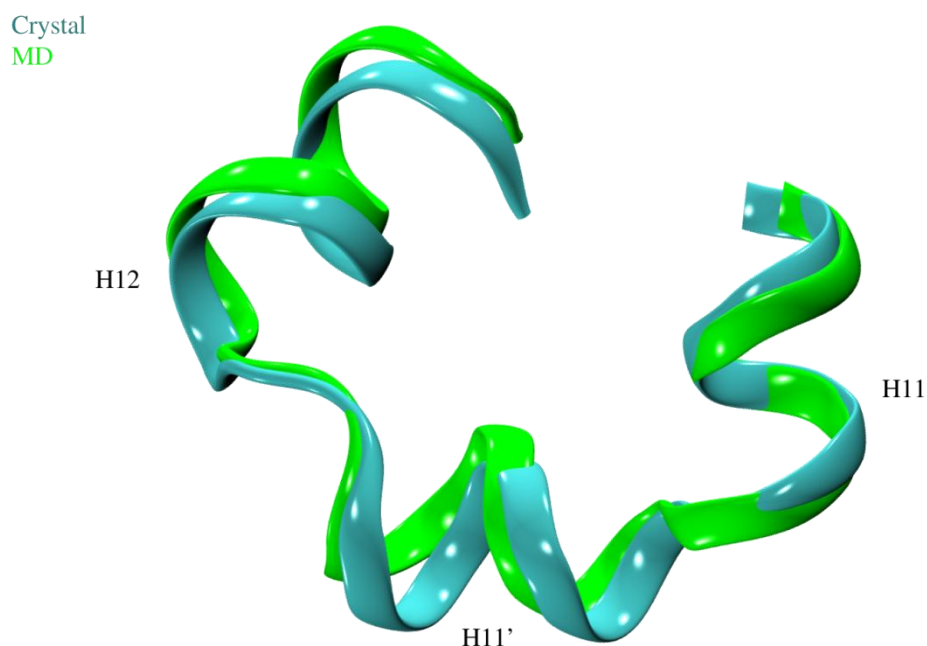
Fig 9: Superimpose of Helix of agonist crystal structure(cyan) and MD stable structure (Orange)

3.5.1 Comparative analysis of structural flexibility and structural transition of Agonist complexes.

The flexibility of residues of Apo and agonist bounded complexes was analyzed using root mean square fluctuation (RMSF) during Molecular dynamic simulation. The RMSF plot provides valuable information about the stability and flexibility of the protein complexes (Fig 10).

Residues with higher RMSF values indicate greater flexibility and reduced stability. Upon binding of agonist the RMSF value of the residues decreased as compared to Apo. In helical region L:H11, H11'/H12 the flexibility of residue were notable lower than apo which indicate that the stability of Helix

12 are in increased which is important for protein activation. The average value of RMSF of Apo and agonist bounded complex was 0.805 and 0.815 respectively.
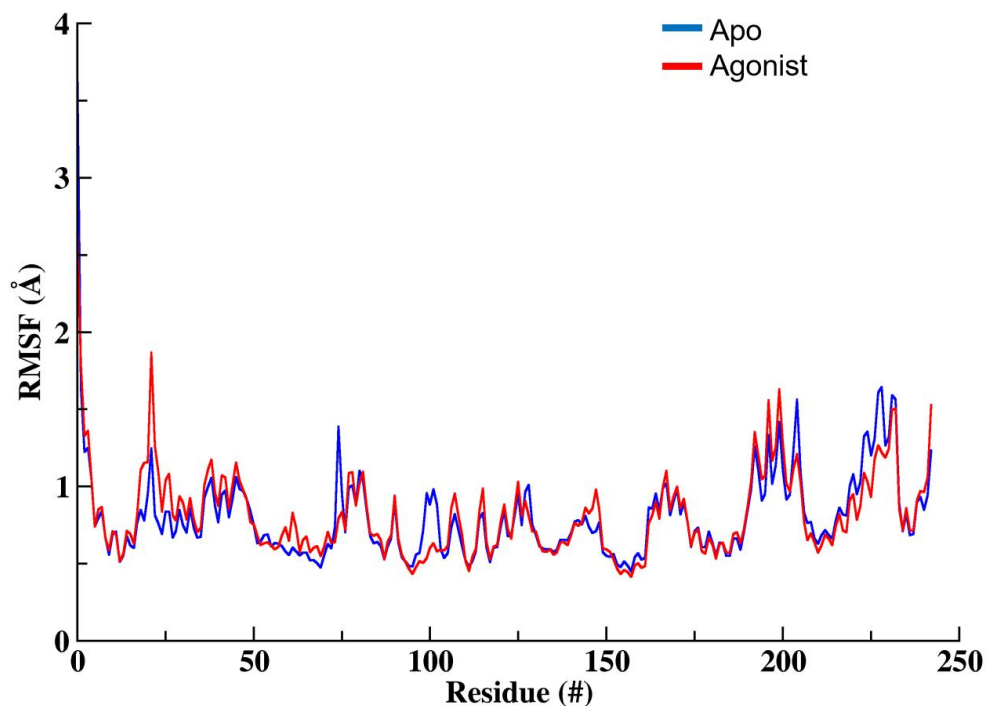
Fig 10: The RMSF graph depicting fluctuation between Apo+coactivator and Protein+Agonist

3.5.2 Comparative analysis of Solvent accessible surface area and compactness of agonist bounded RORγt

Solvent accessible surface area (SASA) measures the solvent accessible surface area of protein and helps to identify the change in protein shape and the exposure of different regions to solvent. Higher SASA value means that more of the molecule is sticking out into solvent, while lower value means that more of the molecule is buried in the protein. SASA was calculated to measure the conformational

changes in hydrophilic and hydrophobic residues. The compactness of the protein was calculated through Radius of Gyration (Rg) analysis. It helps to assess the protein's shape over time.

The Rg plot of Apo and antagonist (Fig 11) bounded RORγt show that initially 150 ns the average Rg of agonist bounded complex is higher than Apo due to the binding of agonist because when ligand bound to protein changes its conformation after 150ns the protein gets stability and the compactness of the protein are similar to the apo protein. The average Rg of agonist-bounded complexes and Apo are 19.01 and 19.04 respectively.
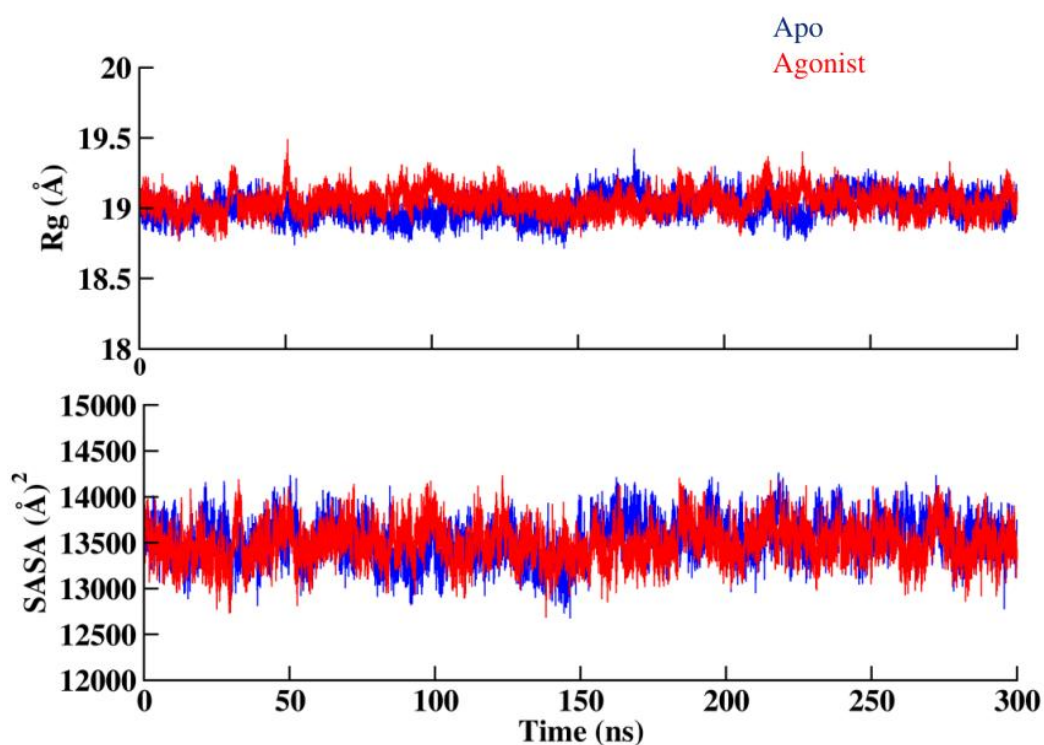
Fig 11:The Rg plot showing the compactness of difference complexes and SASA plot depicting the solvent accessibility of complexes

The SASA graph of apo. and agonist (Fig 11) showed the initally 150ns the antagonist bounded complex display the higher value than Apo which means the suggesting increased exposure of the molecule to the solvent. The higher SASA value may enhance the complex's potential for interaction of other molecules

present in the environment. After 150ns the SASA value are almost similar to Apo SASA value. The average SASA value of agonist bounded complex Apo was 13528 and 13492 respectively.

Overall observation of Rg and SASA indicated that binding of agonist initially changes the protein conformation after gaining stability Rg and SASA value is almost similar to Apo protein.

3.6 Antagonist Crystal vs Dynamic Insights.

To elucidate the dynamic behavior of the antagonist on the RORγt we perform an MD simulation of 300ns. The crystal pose gives a single frame of ligand binding which may change during time intervals to find the behavior of ligands on RORγt protein, MD simulation gives a good idea about that. As compared to the crystal pose and MD stable pose the binding site residues are almost the same but some residues are unique in the crystal pose and MD stable pose. The residues that were unique in crystal pose were ALA368, CYS393 and TYR502 (shown in fig 12). In the MD pose the movement of ligands in the binding pocket residue PHE401, LEU483, ARG 482 are unique. TYR 317 and L362 are indifferent conformation in MD pose shown in Fig 11.
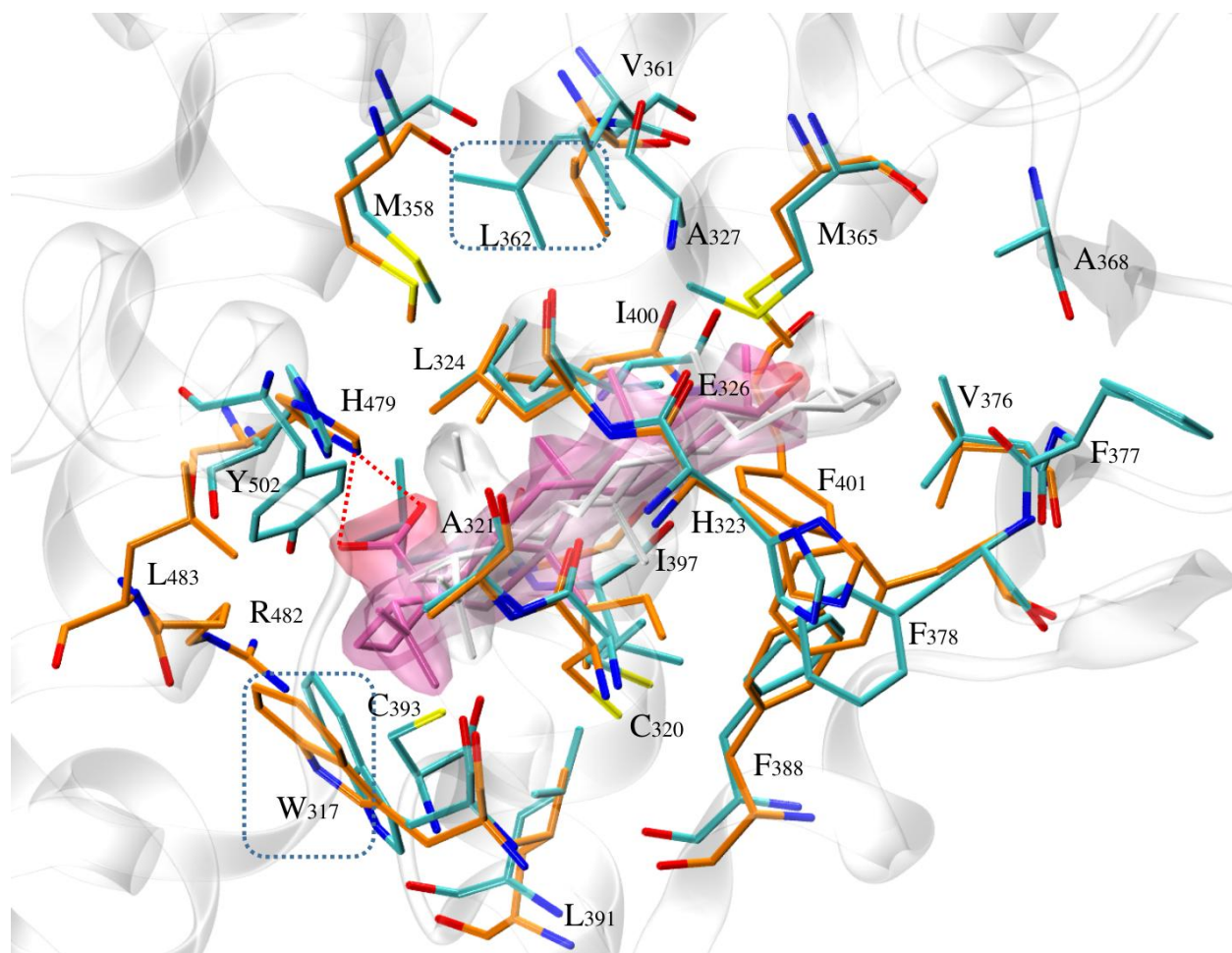
Fig 12: The superimposition of crystal structure binding site residues (cyan)and MD stable pose (orange) indicated that most of the interacting residues have similar conformation. Ligands of crystal structure (white) and MD stable pose (mauve) are shown in licorice. The HBonds are denoted with dashed lines (red) . Blue Dashed lines show the different conformation of residue in MD stable pose.

The dynamic stability of the Antagonist bound RORγt and Apo (shown in fig 13 A) was compared to evaluate the dynamic behaviors of RORγt. The RMSD of the protein of Apo shows an upward trend in the initial 20ns that gets stabilized throughout the simulation. The average RMSD value was 1.488. While in an antagonist bound RORγt protein the RMSD plot showed that it shows an initial 20ns upward trend then it forms a plateau till 3000 ns. The average RMSD value is 1.568. Through RMSD value we conclude that the Proteins are stable in both agonist bound and Apo form.

To elucidate the binding site of RORγt protein after binding with Antagonist we calculate the RMSD of the binding site of Apo and Agonist bounded RORγt protein (shown in fig 13 B). The binding site RMSD plot shows that after binding to the antagonist, RORγt protein, the binding site is stable throughout the simulation. The average RMSD values of the binding site of Apo and agonist-bounded Complex are 1.545 and 1.524 respectively. The average RMSD value of Agonist bounded and Apo are almost similar.
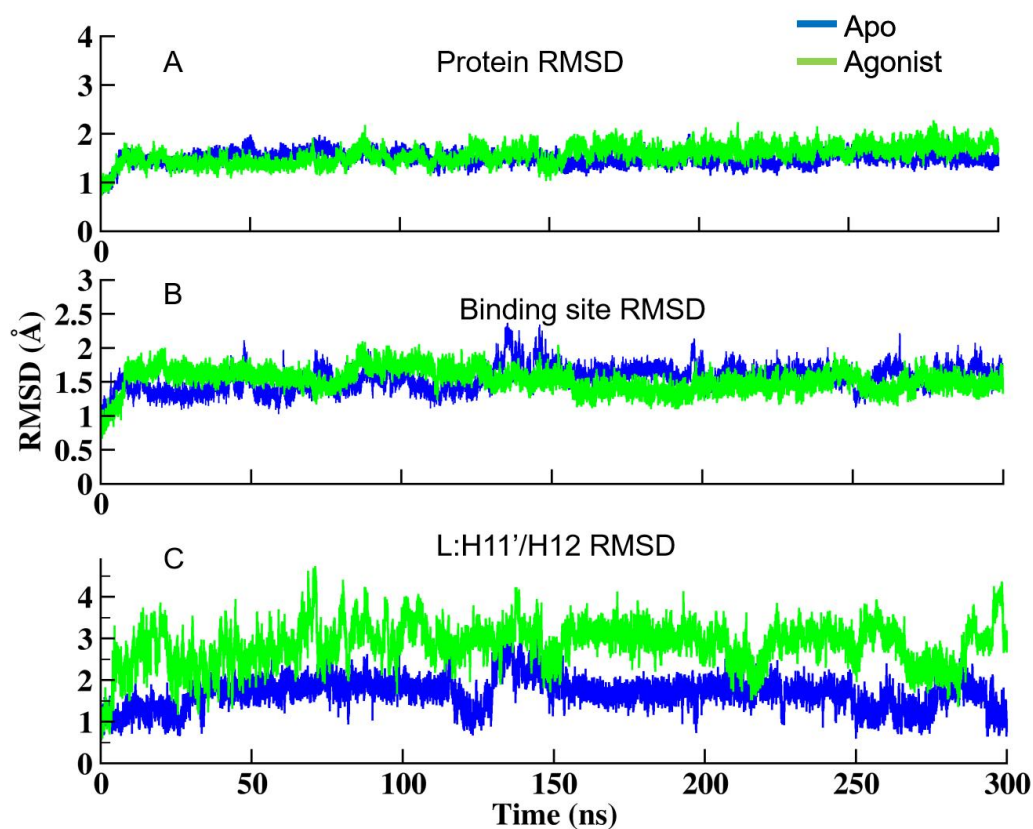
Fig 13: Through molecular dynamics simulations monitoring of time dependent dynamics changes. The RMSD was compared between Apo+coactivator and Protein+Antagonist.

Furthermore, we also calculate the RMSD of L: H11'/H12 (shown in fig 13 C) because L: H11'/H12 are involved in the activation of protein and previous studies show that the after-binding to antagonist L: H11/H12 are destabilized or becomes more flexible. The RMSD Graph of the apo shows that L: H11'/H12 was stable throughout the simulation within the minimum fluctuation due to the C-terminal region. In the Antagonist bounded complex the RMSD plot shows that L: H11'/H12 had more

fluctuations than Apo protein. The RMSD value of antagonist-bounded protein was higher as compared to Apo protein which shows that the L: H11'H12 have more fluctuation than Apo. (shown in fig 14).

Crystal
MD

H12

H11

H11'
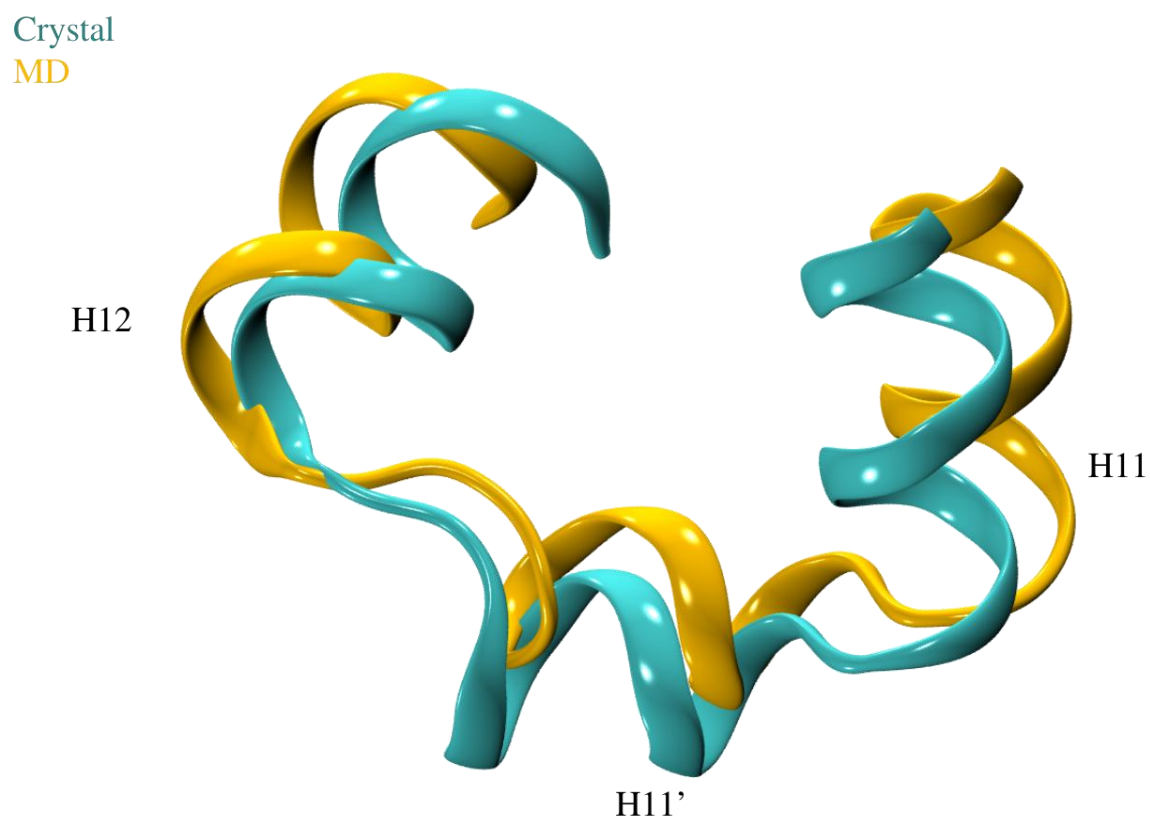
Fig 14: Superimpose of Helix of antagonist crystal structure (cyan) and MD stable structure (orange).

3.6.1 Comparative analysis of structural flexibility and structural transition of Antagonist complexes.

The flexibility of residues of Apo and Antagonist bounded complexes was analyzed using root mean square fluctuation (RMSF) during Molecular dynamic simulation. The RMSF plot provides valuable information about the stability and flexibility of the protein complexes. Residues with higher RMSF values indicate greater flexibility and reduced stability. Upon binding of an Antagonist the RMSF value of the residues increased as compared to Apo (Fig 15).
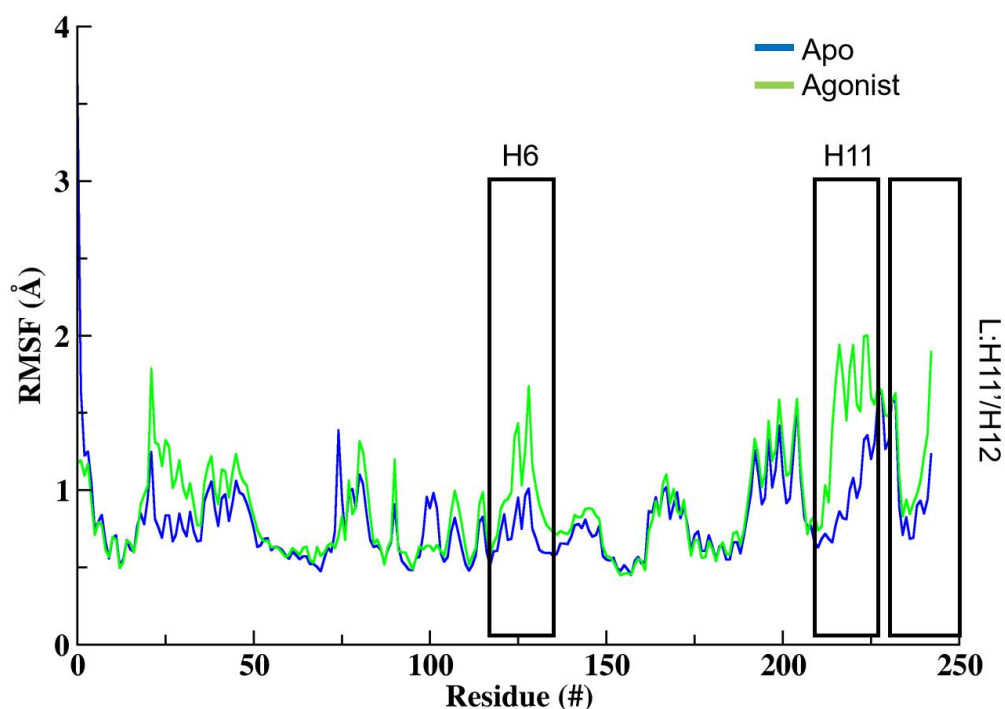
Fig 15: The RMSF was compared between Apo+coactivator and Protein+Antagonist

In helical region H6 and L:H11, H11'/H12 the flexibility of residue is notably higher than apo which indicates that the stability of Helix 12 is decreased which is important for protein activation. The average value of RMSF of Apo and agonist bounded complexes was 0.805 and 0.914 respectively.

3.6.2 Comparative analysis of Solvent accessible surface area and compactness of antagonist bounded RORγt

The Rg plot of Apo and antagonist (Fig 16) bounded RORγt show that initially, 150 ns the average Rg of antagonist bounded complex is higher than Apo due to the binding of antagonist because when ligand bound to a protein it changes its conformation after 150ns the protein gets stability and the compactness of the protein are similar to the apo protein. The average Rg of agonist-bounded complexes and Apo are 19.01 and 19.1 respectively.
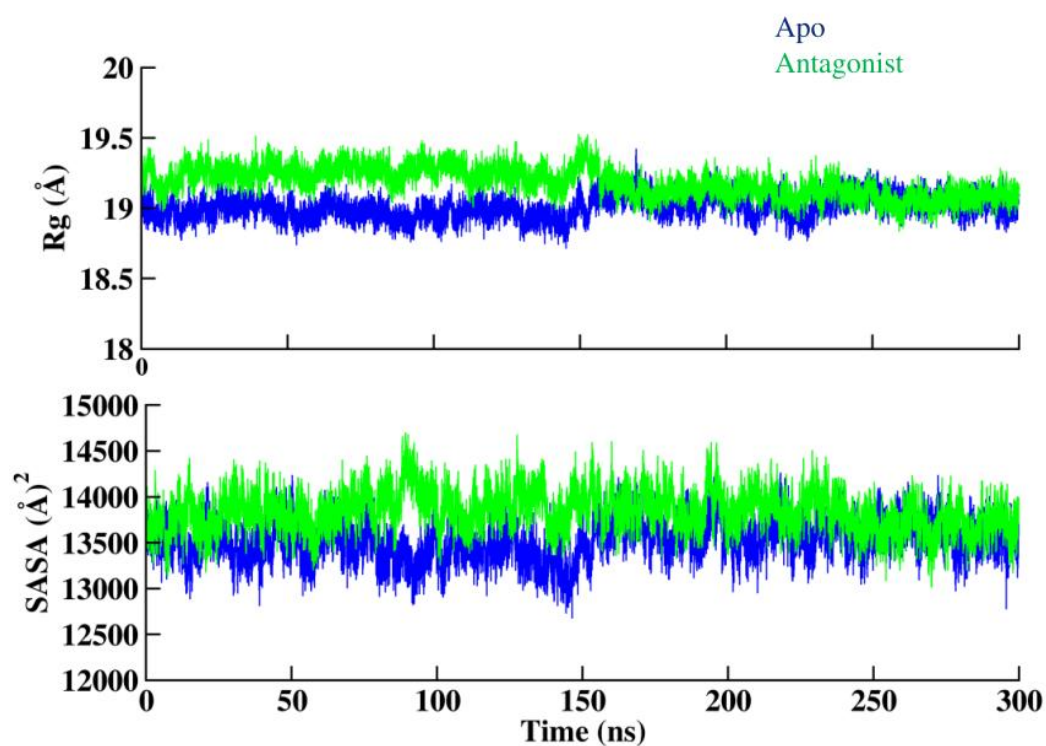
Fig 16: The Rg and SASA plot for Apo+coactivator and Antagonist

The SASA graph of apo and antagonist (Fig 16) showed the initially 150ns the antagonist bounded complex display the higher value than Apo which means the suggesting increased exposure of the molecule to the solvent. The higher SASA value may enhance the complex's potential for interaction of other molecules present in the environment. After 150ns the SASA value are almost similar to Apo

SASA value. The average SASA value of the Antagonist bounded complex Apo was 13528 and 13835 respectively.

Overall observation of Rg and SASA indicated that binding of Antagonist initially changes the protein conformation after gaining stability; its Rg and SASA value is almost similar to Apo protein.

3.7 Dynamic insights of Agonist VS Antagonist

The study of agonists and antagonists has become so important because they bind to the same binding pocket of RORγt protein but their binding effect on the role of RORγt is just the opposite. The binding of agonists activated the RORγt and gene expression occurs in our body, but binding of antagonist in same binding pocket deactivate the RORγt and no gene expression occur. To see the dynamic change occur due to binding of agonist and antagonist we do MD simulation of 300ns of each complex.

The most stable state of the complex was extracted from converged MD simulation for interaction fingerprinting. Firstly, we characterize the binding site residues involved in making Hbond with agonist and antagonist. We calculate the Hbond occupancy throughout the simulation for both the system agonist and antagonist. The PHE377 makes Hbond with occupancy of 44.87% with agonist while in antagonist it forms Hbond with occupancy of 16.41%. Some other residue also formed Hbond throughout the simulation which was shown in Table 6. The Hbond occupancy shows that the PHE 377 makes stronger Hbond bound with agonist throughout the simulation.

Tabel 6: HB Occupancy (Cutoff >5%) of the Interacting Residues with Ligands (agonist/antagonist) in RORγt

Residue number	Ligand ID	occupancy
PHE 377	Agonist	44.87 %
PHE 377	Antagonist	16.41 %
GLU379	Agonist	12.80 %
GLY380	Agonist	6.97 %

To elucidate the change in residue conformation after binding agonist and antagonist we superimpose the stable state of MD of agonist and antagonist. We observed that the L324 plays a major role in the binding of agonist and antagonist, when the agonist binds the L324 is in trans form while when the antagonist binds it changes its conformation from cis to trans. The movement of L324 and weaker Hbond of PHE 377 helps the antagonist bind deep inside the pocket of RORγt. Furthermore, we analyzed the binding site residue (Fig 17) of the agonist and antagonist most of the residue was common. In the agonist complex, the unique residues are GLU 326, ALA 327, ARG 364, ALA 368, and GLU 379 and in the antagonist, the unique residues are LEU 258.
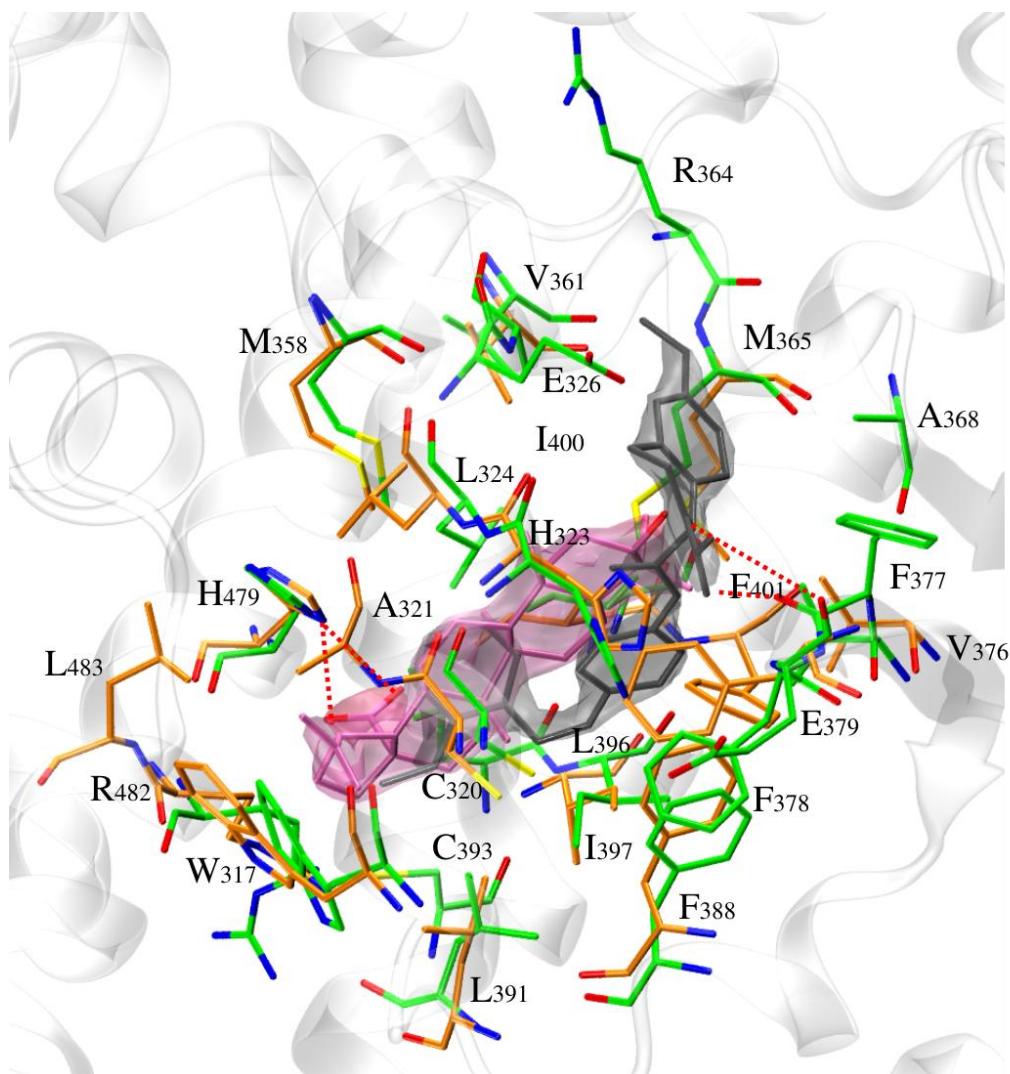
Fig 17: The superimposition of MD stable pose of agonist residue(green) and antagonist residue (orange) binding site. Agonists are shown in gray and antagonists are shown in (mauve) are shown in licorice. The HBonds are denoted with dashed lines (red).

We analyze the movement of residue in the binding site of the agonist and antagonist which are shown in the crystal structure (Fig 3), we observed the that conformation of residue L324, M358, L396, F377, and I397is maintained the crystal conformation throughout the trajectory but some residues like TRP 317, ARG 482 change its conformation during simulation in antagonist while it maintained the crystal conformation in agonist. ARG 482 was shifted outward in the antagonist while in the agonist it maintained its crystal conformation throughout the simulation.
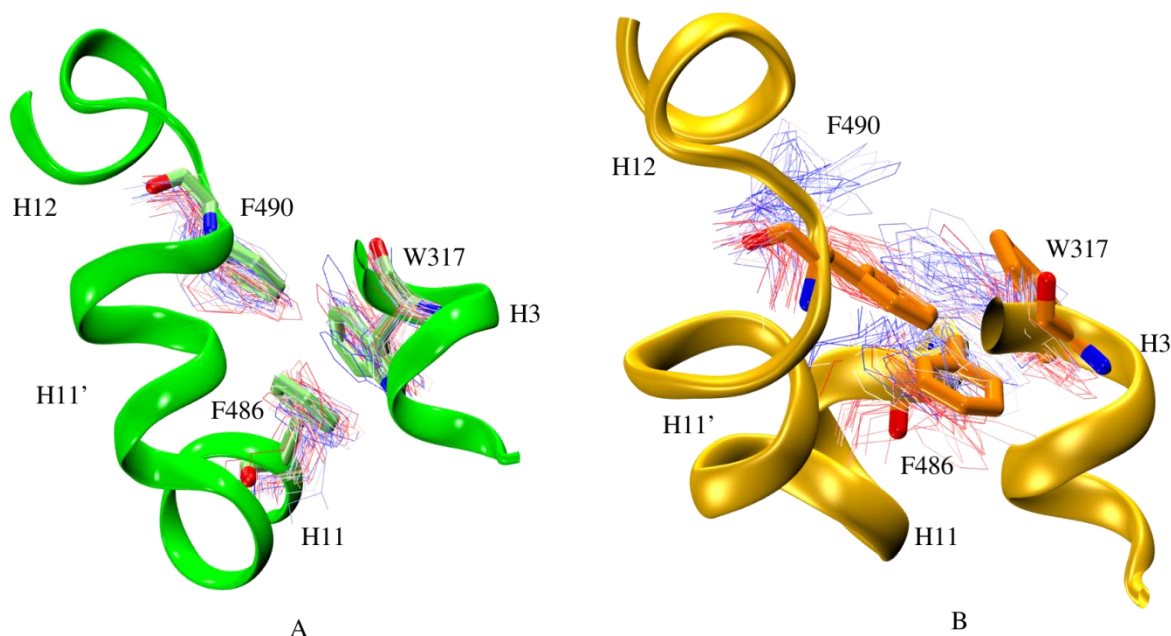
Fig 18: The conformation of the TRP 317 (A) Movement in agonist (green) bounded protein residue with timestep. (B) Movement in antagonist (orange) bounded protein residue with timestep.

The change in the conformation of the TRP 317, lying within H3 helix is though not that great but much enough to cause the disruption between the interactions taking place between the residues present within the helix region H11 and H12 respectively (Fig 18). Consequently, we observed the free movement of the helixH12 after losing the interaction with helix H11 which is also quite evident from the value obtained after RMSD and RMSF analysis.

3.7.1 The dynamic stability of the Agonist bounded RORγt complex and Antagonist bounded complex

The RMSD of protein of Agonist agonist bounded RORγt protein the RMSD plot (Fig 19 A) showed that it shows initial 30ns upward trend then it forms a plateau till 250 ns and then a sudden shift of confirmation. This sudden deviation may occur due to the movement of the loop between Helix 1 and 2. The average RMSD value is 1.36. While in an antagonist bound RORγt protein the RMSD plot showed that it shows an initial 20ns upward trend then it forms a plateau till 3000 ns. The average RMSD value is 1.568
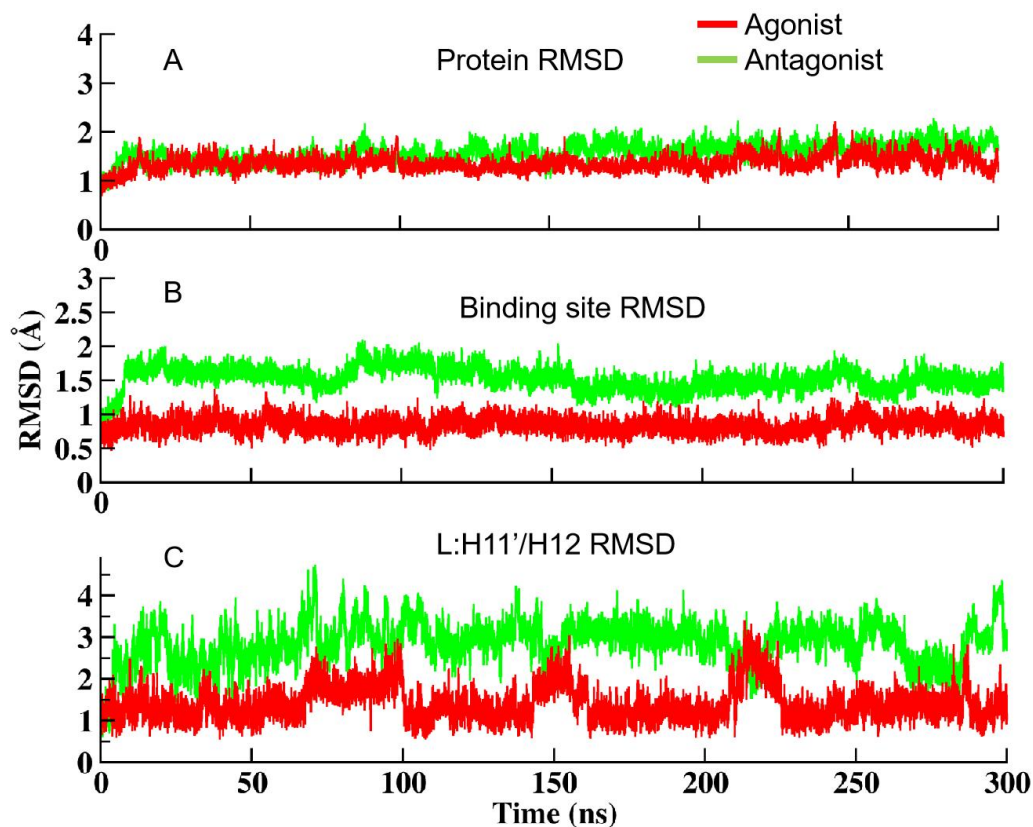
Fig 19: Through molecular dynamics simulations monitoring of time dependent dynamics changes. The RMSD was compared between agonist and antagonist

To elucidate the binding site of RORγt protein after binding with Agonist we calculate the RMSD of the binding site of Agonist bounded complex and antagonist bounded complex protein. The binding site RMSD plot (Fig 19 B) shows that after binding to the agonist RORγt protein the binding site gets more stable than the antagonist complex. In antagonist, the binding site of antagonist was higher RMSD than agonist. The average RMSD values of the binding site of Agonist-bounded complex and antagonist-bounded Complex are 0.815 and 1.524 respectively.

Further, we also calculate the RMSD of L: H11'/H12 because L: H11'/H12 (Fig 19 C) are involved in the activation of protein as previous studies has shown that the after-binding to agonist L: H11/H12 are stabilized. RMSD Graph of the agonist shows that L: H11'/H12 was stable throughout the simulation within the minimum fluctuation due to the C-terminal region. In the antagonist bounded complex the RMSD plot shows that L: H11'/H12 have deviations with time evolution. RMSD of Antagonist is also

stable but value of RMSD of agonist is higher than agonist which indicate that the residues of helical region are more flexible than the agonist.

3.7.2 Comparative analysis of structural flexibility and structural transition of Agonist and Antagonist complexes.

The flexibility of residues of agonist and antagonist bounded complexes was analyzed using root mean square fluctuation (RMSF) during Molecular dynamic simulation. Upon binding of an agonist the RMSF value of the residues decreased as compared to Antagonist binding. In helical region L:H11, H11'/H12 the flexibility of residue is notably lower than Antagonist which indicates that the stability of Helix 12 is higher in agonist bounded as compared to antagonist bounded (Fig 20). The average value of RMSF of the agonist and antagonist bounded complex was 0.815 and 0.914 respectively.
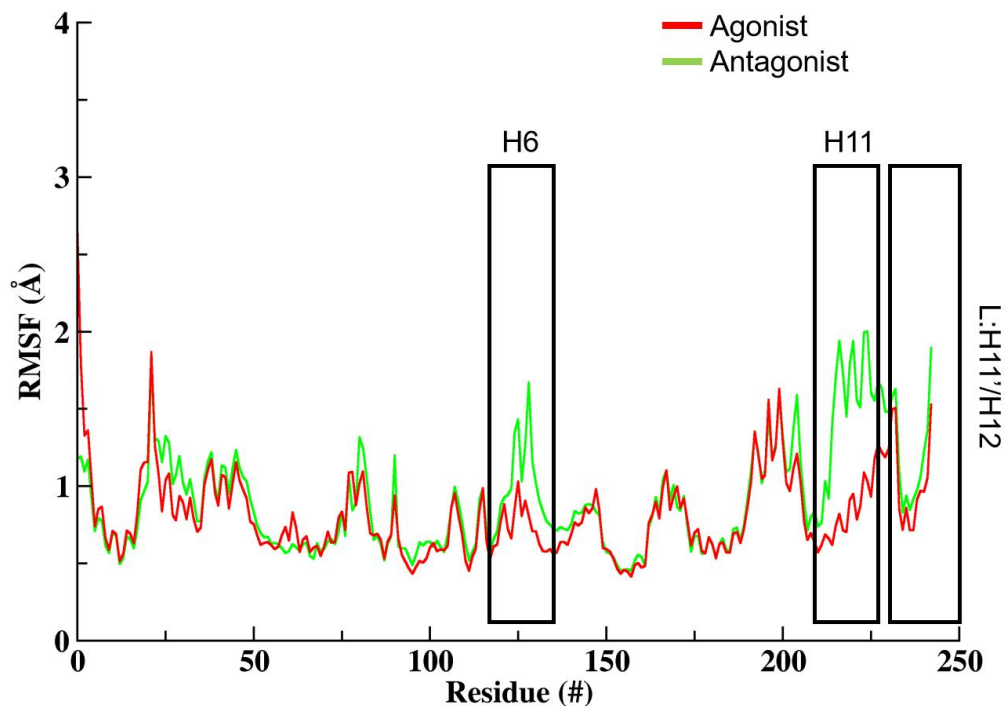
Fig 20: The RMSF plot of protein+agonist and Protein+Antagonist

3.7.3 Comparative analysis of Solvent accessible surface area and compactness of antagonist bounded RORγt

The Rg plot of antagonist bounded RORγt and antagonist bounded complex (Fig 21) show that the initially 150 ns the Rg value of antagonist is higher than the agonist after 150ns when both the complex again their stability and its Rg value is similar. The average values of agonist and antagonist are 19.04 and 19.1 which indicate that the agonist bounded complex were more compact than the antagonist.
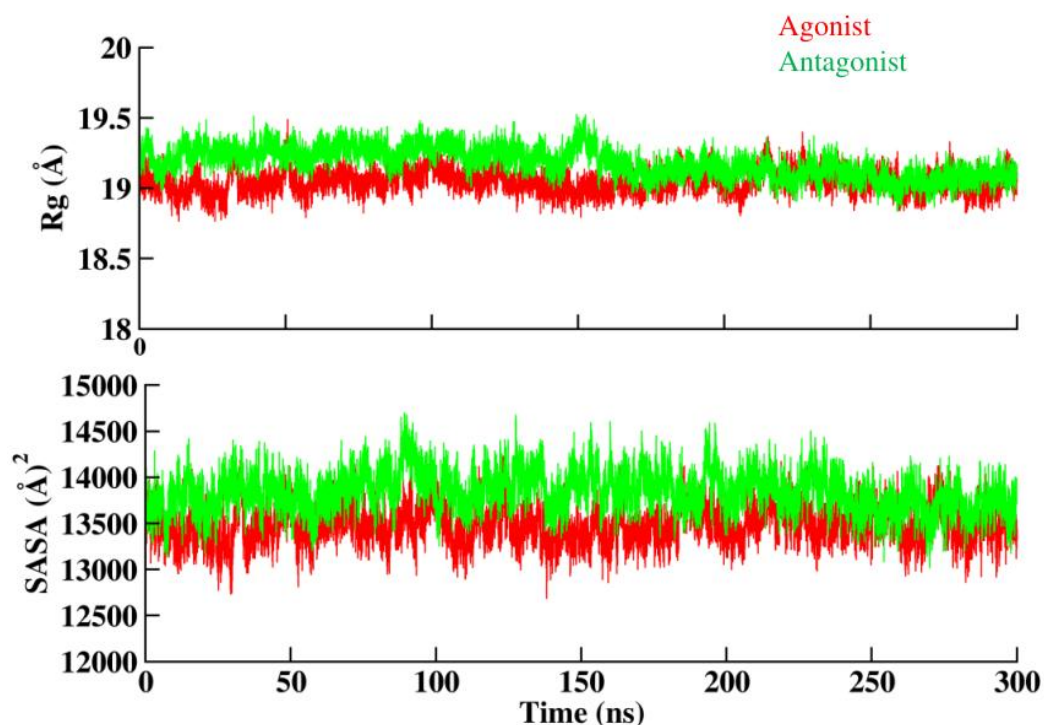
Fig 21: The Rg and SASA plot for Agonist and Antagonist

The SASA graph of agonist bounded complex and antagonist bounded complex (Fig 21) showed the initial 250 ns the antagonist bounded complex display the higher value than agonist which means the suggesting increased exposure of the molecule to the solvent. The higher SASA value may enhance the complex's potential for interaction of other molecules present in the environment. After 250ns the SASA value was almost similar to the agonist SASA value.

3.8 Comparative analysis of Secondary structure between Agonist and Antagonist complexes.

The secondary structure analysis was performed to determine any changes in the protein's secondary structure during simulation. This measures the presence and stability of different secondary structure elements, such as alpha helices and beta sheets. Results of the secondary structure analysis revealed no

significant changes in the secondary structure of Agonist and antagonist complexes. However, in the agonist complex, the transition from alpha helix to
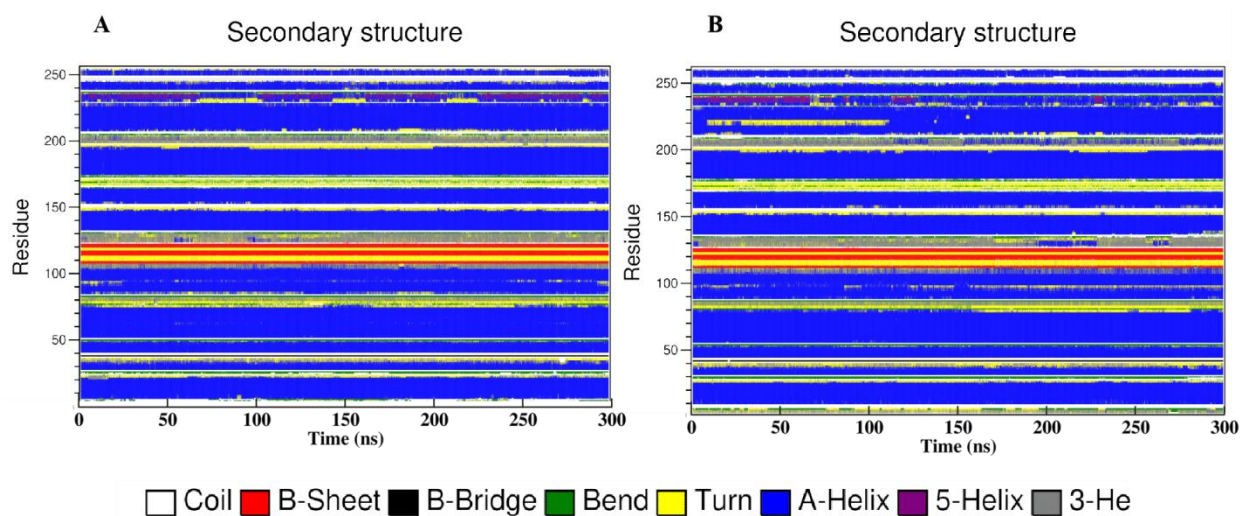
Fig 22: secondary structure plot highlighting the structural transition during simulation of different complexes. (A) secondary structure plot of agonist(B) secondary structure plot of antagonist.

5-helix was observed between residues 231 to 240 (Fig 22 A). While in the antagonist we observed that the transition of helix to 5-helix is minimal as compared to the agonist but in some frames, helix also transitions into turns. In the antagonist complex, the transition of Helix into Turn was observed between residue 229 to 231 (Fig 22 B). In contrast these changes are not observed in the agonist complex.

3.9 Thermodynamic stability and instability of agonist and antagonist complexes.

The MMPBSA approach was used to calculate the binding free energy (ΔG) of agonist and antagonist complexes. The stable trajectories were used to calculate the binding free energies. As expected, the free energy of the agonist (-42.925 kcal/mol) is higher than the antagonist (-32.458 kcal/mol).

This reflects that the binding of the agonist is more energetically favoured than the antagonist. For detailed energy contribution of each critical residue, we performed per-residue decomposition which provides insights into how individual residues contribute to the stabilization of protein-ligand complexes during MD simulation.
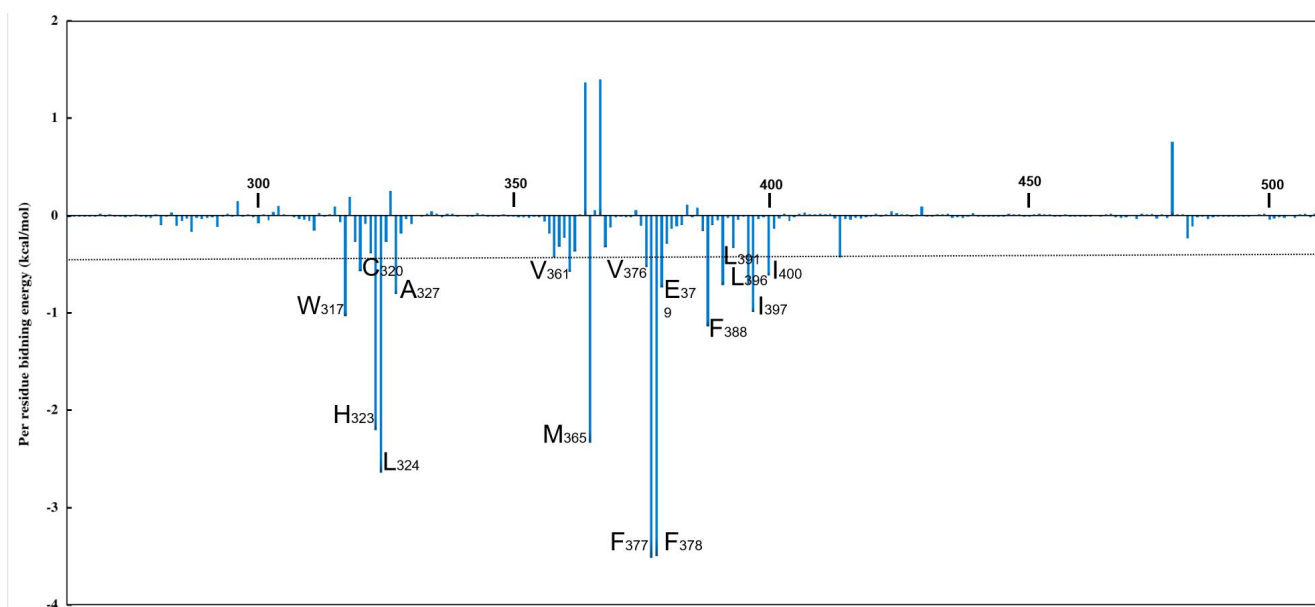
Fig 23: Per residue Energy decomposition analysis of agonist to identify the energetically favorable hot-spot residues.

The calculation was performed on 150 frames extracted from the stable trajectory of each complex. In the agonist complex the energy contribution of RORγt residues as per cutoff was W317, C320, H323, A327, M365, V376, F377, F378, E379, F388, L391, L396, I397, and I400 have shown high energy contribution (shown in Fig 23). While in antagonist complex the energy contribution of RORγt residues as per cutoff was M313, M316, W317, E318, C320, A321, L324, M358, E359, L362, M365, V376, E379, F388, L391 G392, C393, E395, I397, I400, H479, L483, and Y502 have shown high energy contribution (shown in Fig 24).
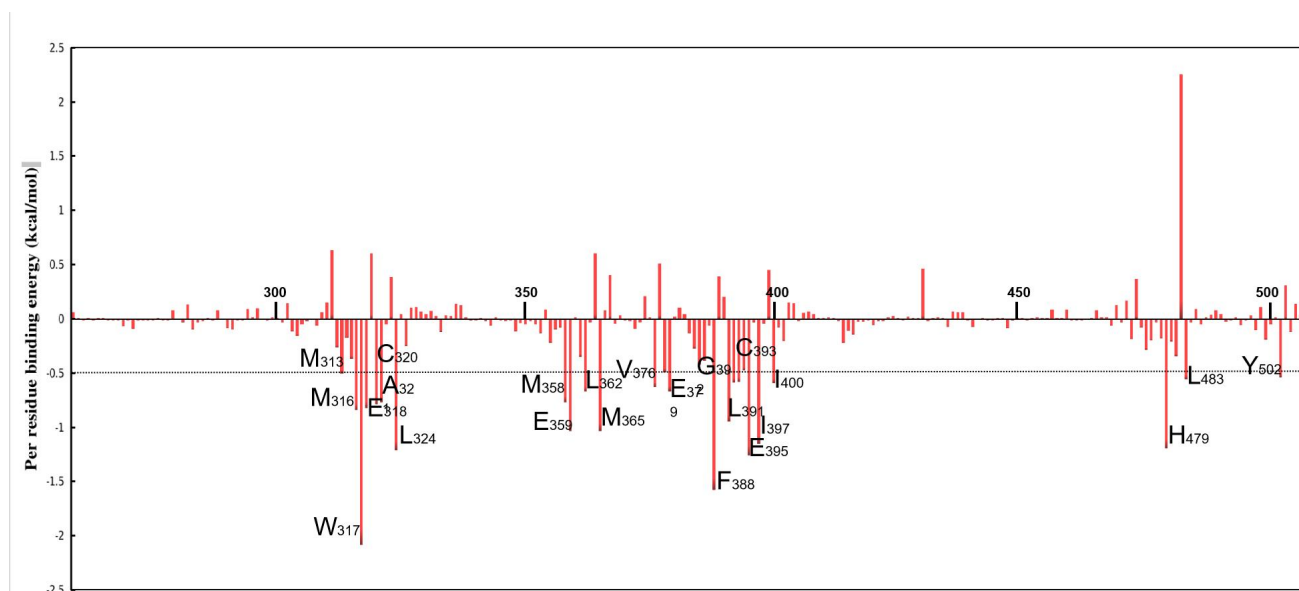
Fig 24: per residue Energy decomposition analysis of antagonist to identify the energetically favorable hot-spot residues.

Some common residues which showed high energy contribution in both complexes are W317, C320, M365, V376, E379, F388, L391, I397 and I400. The strongest interaction energy residue (-3.516, -3.501, -2.644 kcal/mol) is shown by F377, F378, and L324 respectively in agonist and an antagonist the strongest interaction energy residue (-2.08, -1.577, -1. 257) are W317, F388 and E395 respectively. The key residues identified from energy decomposition analysis suggest that Phenylalanine residues play a more significant role in the binding of agonist to RORγt than antagonist. However, tryptophan and methionine play a major role in binding of antagonists to RORγt.

4. Discusson

RORγt agonists and antagonists have attracted extensive attention as novel therapeutic molecules for autoimmune disease and cancer immunotherapy. In our study we discovered the binding mechanism of agonism and antagonists and how the active state of RORγt has been achieved due to conformational changes.

The crystallographic mining followed by MD simulation showed that both agonist and antagonist lead to different conformational change in RORγt. The RMSD and RMSF analysis demonstrate that the ligand alters the dynamics of RORγt differently, and the overall stability varies as it gets reduced in the presence of antagonist than agonist.

From the RMSD of L:H11'/H12 shows that the stability of Helix is reduced or helix is flexible in the presence of an antagonist. Further to the RMSD analysis, we found that the binding of the antagonist has shown residue more flexible in H11, H11'and H12 than antagonist, this result also correlated with RMSD values. Previous studies have reported that the region of L:H11'/H12 are stabilized in the presence of agonists that increase coactivator recruitment. The antagonist is conferred by a kink in H11 that destabilized the L:11'/H12 which destabilized the L:H11'/H12 which is responsible for changing the H12 orientation while with agonist H12 is stable.

We also find that significant conformational change in residue plays a major role in stabilizing the H12. Tryptophan 317 plays a major role in the stability of H12 in the presence of agonists and antagonists. TRP317 present in the binding pocket of RORγt, agonist and antagonist both form hydrophobic contact but in the presence of antagonist TRP317 change is conformation shown in (Fig 18). The movement of TRP317 disrupted the interactions taking place between the residues present within the helix region H11 and H12 respectively; due to this disruption the H12 become more flexible. This also results in a concordance with the RMSF and RMSD findings as well, where the fluctuations in Helix H11 and Loop L:h11'/H12 get reduced in presence of antagonists.

Further, we also performed SASA and ROG to analyze the change in compactness of protein and solvent accessible surface area in presence of agonist and antagonist revealed that the in presence of agonist solvent accessible surface area value are reduced than antagonist due the increase in compactness of protein which also shown in ROG plot.

We further perform thermodynamic quantification to determine the key residues which are involved in the binding of agonists and antagonists. The binding energy of a specific residue is critical for binding of modulator in orthosteric binding pocket. Per residue decomposition revealed that the L324, PHE377, PHE 378 was important for binding agonists. While binding the agonist, the key residue which played a major role was TRP 317, and Methionine. Induced fit results show that L324 also plays a major role in the binding of agonist and antagonist because it changes its conformation in the presence of agonist and antagonist. In the presence of an agonist L324 is in cis conformation while in the presence of an antagonist it changes its conformation from cis to trans form. Hbond occupancy of PHE 377 was 44.87% and 16.41 % throughout simulation in agonist and antagonist respectively which showed that agonist form a strong bond with antagonist rather than antagonist, the per residue binding energy also confirms that of PHE 377 play key role in binding of agonist.

5. Conclusion

The static view of the different RORγt structural conformations and their interactions with different modulators (agonist, antagonist, inverse agonist, and partial agonist) are emphasized by the crystallographic structure structure. Although the crystal structures that are currently available provide crucial insights, there are still several areas that require explanation because they are primarily driven by dynamics. These include the flexibility of RORγt, the properties of the RORγt binding pocket, the molecular recognition mechanism, and the thermodynamics of protein ligand binding. A time-dependent conformational analysis is required to identify the key events and structural determinants in RORγt because the biological modulation of the protein is largely dependent on the substrate (binding of coactivator/corepressor), which primarily drives conformational changes and the beneficial interactions between the sites (catalytic and substrate binding sites).

This study is a comprehensive comparative examination of structural, dynamical and residue level differences between agonists and antagonists that provide novel insights at the atomic level to facilitate the structural-based agonist and antagonist designing. By mining different cocrystals and using Molecular docking and MD simulation, we demarcate the binding sites of RORγt other than the cocrystal binding site and through MD simulation demarcate the conformational dynamics and collective motions of LBD with agonist and antagonist and identified the crucial determinants essential for diverse modulation of RORγt which drive the different biological activity. At structural and residue level, significant conformational changes were observed in RORγt-LBD with agonist and antagonist. From RMSD and RMSF, we have shown that agonists have different motions than agonists partially in L: H11'/H12. Loop and helix regions of H11, H11'and H12 are highly flexible in antagonism, while in agonist Loop and helix regions of H11, H11' and H12 are rigid conformations. The Helix H3 residue W317, L324 and Helix H7 residue L396 and its neighbouring residue I397 and I400 have significant conformational changes in the presence of agonists as it appears that they are possibly responsible for its recruitment. However, the movement of W317 is only seen in case of antagonists. Due to movement W317 in the antagonist disrupted the interactions taking place between the residues present within the helix region H11 and H12 respectively due to this disruption, the H12 became more flexible. This also

results in a concordance with the RMSF and RMSD findings as well, where the fluctuations in Helix H11 and Loop L:h11'/H12 get reduced in the presence of antagonists.

Furthermore, from the thermodynamic analysis, we noticed that that agonist highest binding free energy of -3.516, -3.501, -2.644 kcal/mol is shown by F377, F378, and L324 respectively while in antagonist highest binding -2.08, -1.577, -1. 257 is shown by W317, F388 and E395 respectively are identified to play crucial role for binding of agonist and antagonist respectively.

These findings underscore the pivotal determinants responsible for establishing the residue level communication between two adjacent functional sites of RORγt that is orthosteric binding pocket and coactivator site in presence of agonist and antagonist. Providing evidence of structural rearrangements modulating receptor activation, our structural and functional data expand the mechanistic understanding of RORγt for targeted drug discovery. These results suggest that interaction and communication between orthosteric binding pockets and coactivator binding site (LBD) can possibly be modulated through ligand design as we mapped the pivotal residues and dynamical determinants essential for agonist and antagonist. Dynamic analysis and thermodynamic quantification also suggest that the antagonist is more flexible if the coactivator site (AF2 site) can drive the recruitment of corepressors. Overall, what we have discovered here about the comparative demarcation between agonist and antagonist may help to develop antagonist through structure-guided selective designing, thereby avoiding mechanism-based side effects caused by RORγt activation.

Future Scope of Work

The insights gained from this study on the binding mechanisms and conformational changes of RORγt in the presence of agonists and antagonists gives several promising research directions and potential applications in therapeutic development.

Our detailed analysis of key residues and conformational dynamics provides a solid foundation for designing selective RORγt modulators. Future work can focus on using structure-guided approaches to develop new agonists and antagonists that can precisely modulate RORγt activity, improving therapeutic outcomes for autoimmune diseases and cancers.
High-throughput virtual screening methods can be employed to identify novel compounds that interact with the identified crucial residues (e.g., W317, L324, F377) to either stabilize or destabilize RORγt as needed.

Future studies could involve longer and more complex MD simulations to capture a broader range of dynamic behaviors and interactions of RORγt with different modulators. This could help identify transient states and intermediate conformations that play a role in modulator binding and receptor activation. Enhanced sampling techniques such as metadynamics or accelerated MD could provide deeper insights into the free energy landscapes and transition states of RORγt.

The methodologies and findings of this study can be extended to investigate other nuclear receptors (NRs) that share structural similarities with RORγt. Comparative studies could reveal common mechanisms and unique features across different NRs, aiding in the development of broad-spectrum or highly specific NR modulators. Understanding the interplay between different NRs and their ligands could lead to combination therapies that target multiple pathways involved in disease processes.

The future scope of this work is vast, with opportunities for advancing both fundamental understanding and practical applications. By leveraging our findings, researchers can develop more effective and selective RORγt-targeted therapies, ultimately improving treatment options for patients with autoimmune diseases, cancers, and potentially other conditions influenced by this pivotal nuclear receptor.

References

Berman, H. M., Westbrook, J., Feng, Z., Gilliland, G., Bhat, T. N., Weissig, H., Shindyalov, I. N., &
Bourne, P. E. (2000). The Protein Data Bank. *Nucleic Acids Research*, *28*(1), 235–242.

Bitencourt-Ferreira, G., Pintro, V. O., & de Azevedo, W. F. (2019). Docking with AutoDock4. In W. F.
de Azevedo Jr. (Ed.), *Docking Screens for Drug Discovery* (pp. 125–148). Springer.
https://doi.org/10.1007/978-1-4939-9752-7_9

Blauvelt, A., & Chiricozzi, A. (2018). The Immunologic Role of IL-17 in Psoriasis and Psoriatic
Arthritis Pathogenesis. *Clinical Reviews in Allergy & Immunology*, *55*(3), 379–390.
https://doi.org/10.1007/s12016-018-8702-3

Conti, H. R., Shen, F., Nayyar, N., Stocum, E., Sun, J. N., Lindemann, M. J., Ho, A. W., Hai, J. H., Yu,
J. J., Jung, J. W., Filler, S. G., Masso-Welch, P., Edgerton, M., & Gaffen, S. L. (2009). Th17
cells and IL-17 receptor signaling are essential for mucosal host defense against oral candidiasis.
Journal of Experimental Medicine, *206*(2), 299–311. https://doi.org/10.1084/jem.20081463

Fan, J., Lv, Z., Yang, G., Liao, T. ting, Xu, J., Wu, F., Huang, Q., Guo, M., Hu, G., Zhou, M., Duan, L.,
Liu, S., & Jin, Y. (2018). Retinoic Acid Receptor-Related Orphan Receptors: Critical Roles in
Tumorigenesis. *Frontiers in Immunology*, *9*. https://doi.org/10.3389/fimmu.2018.01187

Fauber, B. P., René, O., de Leon Boenig, G., Burton, B., Deng, Y., Eidenschenk, C., Everett, C., Gobbi,
A., Hymowitz, S. G., Johnson, A. R., La, H., Liimatta, M., Lockey, P., Norman, M., Ouyang, W.,
Wang, W., & Wong, H. (2014). Reduction in lipophilicity improved the solubility, plasma–
protein binding, and permeability of tertiary sulfonamide RORc inverse agonists. *Bioorganic &
Medicinal Chemistry Letters*, *24*(16), 3891–3897. https://doi.org/10.1016/j.bmcl.2014.06.048

Gong, H., Weinstein, D. S., Lu, Z., Duan, J. J.-W., Stachura, S., Haque, L., Karmakar, A., Hemagiri, H., Raut, D. K., Gupta, A. K., Khan, J., Camac, D., Sack, J. S., Pudzianowski, A., Wu, D.-R., Yarde, M., Shen, D.-R., Borowski, V., Xie, J. H., … Dhar, T. G. M. (2018). Identification of bicyclic hexafluoroisopropyl alcohol sulfonamides as retinoic acid receptor-related orphan receptor gamma (RORγ/RORc) inverse agonists. Employing structure-based drug design to improve pregnane X receptor (PXR) selectivity. *Bioorganic & Medicinal Chemistry Letters*, *28*(2), 85–93. https://doi.org/10.1016/j.bmcl.2017.12.006

Harikrishnan, L. S., Gill, P., Kamau, M. G., Qin, L.-Y., Ruan, Z., O'Malley, D., Huynh, T., Stachura, S., Cavallaro, C. L., Lu, Z., J.-W. Duan, J., Weigelt, C. A., Sack, J. S., Ruzanov, M., Khan, J., Gururajan, M., Wong, J. J., Huang, Y., Yarde, M., … Fink, B. E. (2020). Substituted benzyloxytricyclic compounds as retinoic acid-related orphan receptor gamma t (RORγt) agonists. *Bioorganic & Medicinal Chemistry Letters*, *30*(12), 127204. https://doi.org/10.1016/j.bmcl.2020.127204

He, Y.-W., Deftos, M. L., Ojala, E. W., & Bevan, M. J. (1998). RORγt, a Novel Isoform of an Orphan Receptor, Negatively Regulates Fas Ligand Expression and IL-2 Production in T Cells. *Immunity*, *9*(6), 797–806.

Horwitz, K. B., Jackson, T. A., Bain, D. L., Richer, J. K., Takimoto, G. S., & Tung, L. (1996). Nuclear receptor coactivators and corepressors. *Molecular Endocrinology*, *10*(10), 1167–1177. https://doi.org/10.1210/mend.10.10.9121485

Humphrey, W., Dalke, A., & Schulten, K. (1996). VMD: Visual molecular dynamics. *Journal of Molecular Graphics*, *14*(1), 33–38. https://doi.org/10.1016/0263-7855(96)00018-5

Ivanov, I. I., McKenzie, B. S., Zhou, L., Tadokoro, C. E., Lepelley, A., Lafaille, J. J., Cua, D. J., & Littman, D. R. (2006). The Orphan Nuclear Receptor RORγt Directs the Differentiation Program

of Proinflammatory IL-17+ T Helper Cells. *Cell*, *126*(6), 1121–1133. https://doi.org/10.1016/j.cell.2006.07.035

Kallen, J., Izaac, A., Be, C., Arista, L., Orain, D., Kaupmann, K., Guntermann, C., Hoegenauer, K., & Hintermann, S. (2017). Structural States of RORγt: X-ray Elucidation of Molecular Mechanisms and Binding Interactions for Natural and Synthetic Compounds. *ChemMedChem*, *12*(13), 1014–1021. https://doi.org/10.1002/cmdc.201700278

Kanai, T., Mikami, Y., Sujino, T., Hisamatsu, T., & Hibi, T. (2012). RORγt-dependent IL-17A-producing cells in the pathogenesis of intestinal inflammation. *Mucosal Immunology*, *5*(3), 240–247. https://doi.org/10.1038/mi.2012.6

Khan, D., & Ansar Ahmed, S. (2015). Regulation of IL-17 in autoimmune diseases by transcriptional factors and microRNAs. *Frontiers in Genetics*, *6*. https://doi.org/10.3389/fgene.2015.00236

Kono, M., Ochida, A., Oda, T., Imada, T., Banno, Y., Taya, N., Masada, S., Kawamoto, T., Yonemori, K., Nara, Y., Fukase, Y., Yukawa, T., Tokuhara, H., Skene, R., Sang, B.-C., Hoffman, I. D., Snell, G. P., Uga, K., Shibata, A., … Yamamoto, S. (2018). Discovery of [cis-3-({(5R)-5-[(7-Fluoro-1,1-dimethyl-2,3-dihydro-1H-inden-5-yl)carbamoyl]-2-methoxy-7,8-dihydro-1,6-naphthyridin-6(5H)-yl}carbonyl)cyclobutyl]acetic Acid (TAK-828F) as a Potent, Selective, and Orally Available Novel Retinoic Acid Receptor-Related Orphan Receptor γt Inverse Agonist. *Journal of Medicinal Chemistry*, *61*(7), 2973–2988. https://doi.org/10.1021/acs.jmedchem.8b00061

Kumari, A., Mittal, L., Srivastava, M., & Asthana, S. (2022). Binding mode characterization of 13b in the monomeric and dimeric states of SARS-CoV-2 main protease using molecular dynamics simulations. *Journal of Biomolecular Structure and Dynamics*, *40*(19), 9287–9305. https://doi.org/10.1080/07391102.2021.1927844

Kumari, A., Mittal, L., Srivastava, M., Pathak, D. P., & Asthana, S. (2023). Deciphering the Structural

    Determinants Critical in Attaining the FXR Partial Agonism. *The Journal of Physical Chemistry*

    B, *127*(2), 465–485. https://doi.org/10.1021/acs.jpcb.2c06325

Li, X., Anderson, M., Collin, D., Muegge, I., Wan, J., Brennan, D., Kugler, S., Terenzio, D., Kennedy,

    C., Lin, S., Labadia, M. E., Cook, B., Hughes, R., & Farrow, N. A. (2017). Structural studies

    unravel the active conformation of apo RORγt nuclear receptor and a common inverse agonism

    of two diverse classes of RORγt inhibitors. *Journal of Biological Chemistry*, *292*(28), 11618–

    11630. https://doi.org/10.1074/jbc.M117.789024

Lu, Z., Duan, J. J.-W., Xiao, H., Neels, J., Wu, D.-R., Weigelt, C. A., Sack, J. S., Khan, J., Ruzanov, M.,

    An, Y., Yarde, M., Karmakar, A., Vishwakrishnan, S., Baratam, V., Shankarappa, H., Vanteru,

    S., Babu, V., Basha, M., Kumar Gupta, A., … Murali Dhar, T. G. (2019). Identification of potent,

    selective and orally bioavailable phenyl ((*R*)-3-phenylpyrrolidin-3-yl)sulfone analogues as

    RORγt inverse agonists. *Bioorganic & Medicinal Chemistry Letters*, *29*(16), 2265–2269.

    https://doi.org/10.1016/j.bmcl.2019.06.036

Marcotte, D. J., Liu, Y., Little, K., Jones, J. H., Powell, N. A., Wildes, C. P., Silvian, L. F., &

    Chodaparambil, J. V. (2016). Structural determinant for inducing RORgamma specific inverse

    agonism triggered by a synthetic benzoxazinone ligand. *BMC Structural Biology*, *16*(1), 7.

    https://doi.org/10.1186/s12900-016-0059-3

McEwan, I. J. (2009). Nuclear Receptors: One Big Family. In I. J. McEwan (Ed.), *The Nuclear Receptor*

    Superfamily: Methods and Protocols (pp. 3–18). Humana Press. https://doi.org/10.1007/978-1-

    60327-575-0_1

Mei, L., Xu, L., Wu, S., Wang, Y., Xu, C., Wang, L., Zhang, X., Yu, C., Jiang, H., Zhang, X., Bai, F., &

    Xie, C. (2023). Discovery, structural optimization, and anti-tumor bioactivity evaluations of

betulinic acid derivatives as a new type of RORγ antagonists. *European Journal of Medicinal Chemistry*, *257*, 115472. https://doi.org/10.1016/j.ejmech.2023.115472

Noguchi, M., Nomura, A., Murase, K., Doi, S., Yamaguchi, K., Hirata, K., Shiozaki, M., Hirashima, S., Kotoku, M., Yamaguchi, T., Katsuda, Y., Steensma, R., Li, X., Tao, H., Tse, B., Fenn, M., Babine, R., Bradley, E., Crowe, P., … Kamada, M. (2017). Ternary complex of human RORγ ligand-binding domain, inverse agonist and SMRT peptide shows a unique mechanism of corepressor recruitment. *Genes to Cells*, *22*(6), 535–551. https://doi.org/10.1111/gtc.12494

Oh, T. G., Wang, S.-C. M., Acharya, B. R., Goode, J. M., Graham, J. D., Clarke, C. L., Yap, A. S., & Muscat, G. E. O. (2016). The Nuclear Receptor, RORγ, Regulates Pathways Necessary for Breast Cancer Metastasis. *EBioMedicine*, *6*, 59–72. https://doi.org/10.1016/j.ebiom.2016.02.028

Park, T.-Y., Park, S.-D., Cho, J.-Y., Moon, J.-S., Kim, N.-Y., Park, K., Seong, R. H., Lee, S.-W., Morio, T., Bothwell, A. L. M., & Lee, S.-K. (2014). RORγt-specific transcriptional interactomic inhibition suppresses autoimmunity associated with TH17 cells. *Proceedings of the National Academy of Sciences*, *111*(52), 18673–18678. https://doi.org/10.1073/pnas.1413687112

Parrado, A., Despouy, G., Kraïba, R., Pogam, C. L., Dupas, S., Choquette, M., Robledo, M., Larghero, J., Bui, H., Gall, I. L., Rochette-Egly, C., Chomienne, C., & Padua, R. A. (2001). Retinoic acid receptor α1 variants, RARα1ΔB and RARα1ΔBC, define a new class of nuclear receptor isoforms. *Nucleic Acids Research*, *29*(24), 4901–4908.

Rutz, S., Eidenschenk, C., Kiefer, J. R., & Ouyang, W. (2016). Post-translational regulation of RORγt— A therapeutic target for the modulation of interleukin-17-mediated responses in autoimmune diseases. *Cytokine & Growth Factor Reviews*, *30*, 1–17. https://doi.org/10.1016/j.cytogfr.2016.07.004

Shi, Q., Xiao, Z., Yang, M. G., Marcoux, D., Cherney, R. J., Yip, S., Li, P., Wu, D.-R., Weigelt, C. A., Sack, J., Khan, J., Ruzanov, M., Wang, J., Yarde, M., Ellen Cvijic, M., Li, S., Shuster, D. J., Xie, J., Sherry, T., … Dhar, T. G. M. (2020). Tricyclic sulfones as potent, selective and efficacious RORγt inverse agonists – Exploring C6 and C8 SAR using late-stage functionalization. *Bioorganic & Medicinal Chemistry Letters*, *30*(23), 127521. https://doi.org/10.1016/j.bmcl.2020.127521

Strutzenberg, T. S., Garcia-Ordonez, R. D., Novick, S. J., Park, H., Chang, M. R., Doebellin, C., He, Y., Patouret, R., Kamenecka, T. M., & Griffin, P. R. (2019). Correction: HDX-MS reveals structural determinants for RORγ hyperactivation by synthetic agonists. *eLife*, *8*, e52847. https://doi.org/10.7554/eLife.52847

Suri, C., Awasthi, A., & Asthana, S. (2022). Crystallographic landscape provides molecular insights into the modes of action of diverse ROR-γt modulators. *Drug Discovery Today*, *27*(2), 652–663. https://doi.org/10.1016/j.drudis.2021.11.022

van Niel, M. B., Fauber, B. P., Cartwright, M., Gaines, S., Killen, J. C., René, O., Ward, S. I., de Leon Boenig, G., Deng, Y., Eidenschenk, C., Everett, C., Gancia, E., Ganguli, A., Gobbi, A., Hawkins, J., Johnson, A. R., Kiefer, J. R., La, H., Lockey, P., … Wong, H. (2014). A reversed sulfonamide series of selective RORc inverse agonists. *Bioorganic & Medicinal Chemistry Letters*, *24*(24), 5769–5776. https://doi.org/10.1016/j.bmcl.2014.10.037

Wang, T., Banerjee, D., Bohnert, T., Chao, J., Enyedy, I., Fontenot, J., Guertin, K., Jones, H., Lin, E. Y., Marcotte, D., Talreja, T., & Van Vloten, K. (2015). Discovery of novel pyrazole-containing benzamides as potent RORγ inverse agonists. *Bioorganic & Medicinal Chemistry Letters*, *25*(15), 2985–2990. https://doi.org/10.1016/j.bmcl.2015.05.028

Wang, Y., Cai, W., Tang, T., Liu, Q., Yang, T., Yang, L., Ma, Y., Zhang, G., Huang, Y., Song, X., Orband-Miller, L. A., Wu, Q., Zhou, L., Xiang, Z., Xiang, J.-N., Leung, S., Shao, L., Lin, X., Lobera, M., & Ren, F. (2018). From RORγt Agonist to Two Types of RORγt Inverse Agonists. *ACS Medicinal Chemistry Letters*, *9*(2), 120–124. https://doi.org/10.1021/acsmedchemlett.7b00476

Wang, Y., Yang, T., Liu, Q., Ma, Y., Yang, L., Zhou, L., Xiang, Z., Cheng, Z., Lu, S., Orband-Miller, L. A., Zhang, W., Wu, Q., Zhang, K., Li, Y., Xiang, J.-N., Elliott, J. D., Leung, S., Ren, F., & Lin, X. (2015). Discovery of *N*-(4-aryl-5-aryloxy-thiazol-2-yl)-amides as potent RORγt inverse agonists. *Bioorganic & Medicinal Chemistry*, *23*(17), 5293–5302. https://doi.org/10.1016/j.bmc.2015.07.068

Weikum, E. R., Liu, X., & Ortlund, E. A. (2018). The nuclear receptor superfamily: A structural perspective. *Protein Science : A Publication of the Protein Society*, *27*(11), 1876–1892. https://doi.org/10.1002/pro.3496

Yang, T., Liu, Q., Cheng, Y., Cai, W., Ma, Y., Yang, L., Wu, Q., Orband-Miller, L. A., Zhou, L., Xiang, Z., Huxdorf, M., Zhang, W., Zhang, J., Xiang, J.-N., Leung, S., Qiu, Y., Zhong, Z., Elliott, J. D., Lin, X., & Wang, Y. (2014). Discovery of Tertiary Amine and Indole Derivatives as Potent RORγt Inverse Agonists. *ACS Medicinal Chemistry Letters*, *5*(1), 65–68. https://doi.org/10.1021/ml4003875

Yukawa, T., Nara, Y., Kono, M., Sato, A., Oda, T., Takagi, T., Sato, T., Banno, Y., Taya, N., Imada, T., Shiokawa, Z., Negoro, N., Kawamoto, T., Koyama, R., Uchiyama, N., Skene, R., Hoffman, I., Chen, C.-H., Sang, B., … Shirai, J. (2019). Design, Synthesis, and Biological Evaluation of Retinoic Acid-Related Orphan Receptor γt (RORγt) Agonist Structure-Based Functionality

Switching Approach from In House RORγt Inverse Agonist to RORγt Agonist. *Journal of Medicinal Chemistry*, *62*(3), 1167–1179. https://doi.org/10.1021/acs.jmedchem.8b01181

Zenobia, C., & Hajishengallis, G. (2015). Basic biology and role of interleukin-17 in immunity and inflammation. *Periodontology 2000*, *69*(1), 142–159. https://doi.org/10.1111/prd.12083

Zhang, Y., Luo, X., Wu, D., & Xu, Y. (2015). ROR nuclear receptors: Structures, related diseases, and drug discovery. *Acta Pharmacologica Sinica*, *36*(1), 71–87. https://doi.org/10.1038/aps.2014.120

Zhu, J., Yamane, H., & Paul, W. E. (2010). Differentiation of Effector CD4 T Cell Populations*. *Annual Review of Immunology*, *28*(Volume 28, 2010), 445–489. https://doi.org/10.1146/annurev-immunol-030409-101212

Zou, W., & Restifo, N. P. (2010). TH17 cells in tumour immunity and immunotherapy. *Nature Reviews Immunology*, *10*(4), 248–256. https://doi.org/10.1038/nri2742